# Phase Separation of Polymer Mixtures in the Presence of Solvent

**A. Sariban and K. Binder***

*Institut für Physik, Johannes-Gutenberg-Universität Mainz, D-6500 Mainz, Postfach 3980, Federal Republic of Germany.* *Received July 10, 1987; Revised Manuscript Received September 10, 1987*

ABSTRACT: A model of a symmetrical polymer mixture, where both polymers A and B are modeled by self-avoiding walks of $N_A = N_B = N$ steps on the simple cubic lattice and a lattice site is taken by either an A monomer, a B monomer, or a solvent molecule (or a vacancy V, respectively), is analyzed by Monte Carlo simulations, in order to analyze the validity of the predictions of the Flory–Huggins theory. We introduce energy parameters $\epsilon \equiv \epsilon_{AA} = \epsilon_{BB}$ if two neighboring sites are taken by monomers of the same kind and $\epsilon_{AB}$ if they are taken by monomers of different kind, while energy parameters involving the solvent (or vacancies) are put equal to zero. Solvent concentrations $\phi_v = 0.2$, 0.4, 0.6, and 0.8 and chain lengths $N = 4$, 8, 16, 32, and 64 are considered. It is shown that the linear dimensions of the chains in this concentrated solution regime still have a pronounced dependence on both concentration and temperature, the minority component having systematically smaller radii (although for $\epsilon = \epsilon_{AB} = 0$ both A and B have identical radii). We attribute the huge discrepancies found between the "exact" critical temperature of phase separation for this model and those predicted by the Flory–Huggins approximation to the crude treatment of chain configurational statistics in this approximation. We also obtain binodal curves and the scattering function $S_{coll}(q \to 0)$ and discuss the crossover from Ising-like critical behavior to mean-field critical behavior as $N \to \infty$. Consequences for experimental work are briefly discussed.

## 1. Introduction

There exists an enormous amount of literature on the thermodynamic properties of polymer solutions and polymer blends, which is based on the Flory–Huggins lattice model[1-26] or generalizations thereof, such as the Sanchez–Lacombe lattice fluid model;[27] these theories are broadly accepted for the interpretation of experimental data.

It has been well-known for a long time, of course, that these theories involve drastic approximations even beyond the use of a lattice model [which may be inappropriate for a fluid system, particularly if there exists a pronounced disparity in the size and shape of the monomeric units (and the solvent molecules, if they are included)]. In fact, there are three kinds of approximations: First, in the treatment of the pairwise interaction between monomers of polymer A and polymer B, one neglects any correlations in the occupation probability of lattice sites; this leads to an expression of the interaction enthalpy of the form $\chi\Phi_A\Phi_B$ where $\chi$ is a "Flory–Huggins parameter" and $\Phi_A$ and $\Phi_B$ are the volume fractions of A and B monomers, respectively. For symmetric polymer mixtures ($N_A = N_B = N$) the Flory–Huggins theory[1-8] predicts the critical point of unmixing to occur for $\chi = \chi_c = 2/[(1 - \phi_v)N]$, where $\phi_v$ is the volume fraction of the solvent (or vacancies, respectively). Since $\chi_c \to 0$ for $N \to \infty$, it is clear that this weak interaction should not introduce strong correlations in the occupation probability, and hence this mean-field approximation is believed to be rather accurate.[28,29,17] Second, for estimation of the configurational entropy of the chains, most of the excluded volume restrictions are neglected. While for dense polymer systems the excluded volume interaction should "cancel out" in the sense that[1,28] the relation for the gyration radius $\langle R^2_{gyr} \rangle \propto N$ holds asymptotically for large $N$, the prefactor in this relation is larger than the prefactor for simple random walks: thus, the accuracy of the expression for the configurational entropy per lattice site[1-8]

$$S/k_B = \frac{\phi_A \ln \phi_A}{N_A} + \frac{\phi_B \ln \phi_B}{N_B} + \phi_v \ln \phi_v \qquad (1)$$

is not obvious. The third approximation involves the relation between the Flory–Huggins parameter $\chi$ and the nearest-neighbor pair energies $\epsilon_{AA}$, $\epsilon_{BB}$, and $\epsilon_{AB}$ (between two A monomers, two B monomers, or one A and one B monomer, respectively) where one chooses[1]

$$\chi = \frac{z(2\epsilon_{AB} - \epsilon_{AA} - \epsilon_{BB})}{2k_BT} \qquad (2)$$

with $z$ being the coordination number of the lattice. Clearly, eq 2 only holds for $z \to \infty$ as at most $z - 2$ neighboring sites of an inner monomer can be available for occupation by monomers of *other* chains.

Attempts[12-14] to find improved analytical expressions for both $S$ and $\chi$ have appeared already in the early literature,[12,13] but the common belief[1,27] is that such improvements are not really necessary: thus, the simple Flory–Huggins expression for the Gibbs free energy of mixing (which we write down here for $\phi_v = 0$ only)

$$\frac{\Delta G}{k_BT} = \frac{\phi_A \ln \phi_A}{N_A} + \frac{\phi_B \ln \phi_B}{N_B} + \chi\phi_A\phi_B \qquad (3)$$

has been the standard starting point for generalizations considering ternary[6,10,11] or multicomponent[8] mixtures, unmixing kinetics,[15-18] interfacial structure,[19-25] block copolymers,[26] etc. Comparing such work to corresponding experimental data does not provide a clear-cut test of the theory, since the Flory–Huggins lattice model is a crude oversimplification of nature, and it is not obvious to give a precise meaning to its basic microscopic parameters (lattice constant $a$, coordination number $z$, energy parameters $\phi_{AA}$, $\phi_{BB}$, $\phi_{AB}$, etc.). Thus, while there is a rich literature where eq 3 (or generalizations thereof[27]) is fitted to some experimental data and the temperature and concentration dependence of $\chi$ are extracted,[8,27,30,31] it is not clear to what extent this behavior of $\chi$ represents real physics and to what extent it represents simply artifacts due to inaccurate statistical mechanics involved in the derivation of eq 1–3.

In the present paper we shall present a more crucial test of the Flory–Huggins theory, by performing Monte Carlo simulations[32-34] of the Flory–Huggins lattice model including a solvent (or vacancies V). In this approach, the microscopic parameters of the Flory–Huggins theory have a precise meaning, but the three crude approximations above are avoided: the Monte Carlo method[32-34] provides the "numerically exact" statistical mechanics of the model, apart from statistical errors and systematic errors due to

0024-9297/88/2221-0711$01.50/0 

finite lattice size, etc.,[32,33] which can be controlled, however. In previous work[35,36] we have demonstrated the feasibility of this approach by studying one value of $\phi_v$ only, $\phi_v = 0.2$; in the present paper we extend this work and study the variation[37,38] of the properties of the model with increasing $\phi_v$, including also larger chain lengths ($N = 64$). Unexpectedly, we find that for rather concentrated solutions ($\phi_v = 0.2$–$0.8$) the excluded volume effects present on short length scales seems to be rather important in explaining the actual properties of the model.

In section 2 we briefly recall the simulation method[36] and, as an example, present "raw data" for the cases $N = 64$, $\phi_v = 0.6$ and $N = 16$, $\phi_v = 0.8$ and their analysis by "finite-size scaling" techniques.[39–41] Section 3 then shows results for the equation of state of the mixture for various vacancy concentrations and discusses the critical temperature for phase separation as a function of both $\phi_v$ and $N$, comparing it to theoretical predictions. Section 4 then shows results for the chain linear dimensions as a function of temperature and concentration and presents a tentative interpretation of our findings, incorporating excluded volume effects into the treatment of the de Gennes[28] random-phase approximation. Section 5, finally, summarizes our conclusions and discusses pertinent experimental work.

## 2. Simulation Technique and Analysis of the "Raw Data" Obtained by the Monte Carlo Method

An extensive description of our techniques and their application to the Flory–Huggins model has already been given elsewhere,[36] and hence here we are summarizing the main points only.

We study simple cubic $L \times L \times L$ lattices, with box linear dimensions between $L = 8$ and $L = 30$ lattice spacings, applying periodic boundary conditions. We are studying here only symmetric mixtures ($N_A = N_B = N$); all polymer chains are represented as random walks on the lattice. These random walks are both self-avoiding and mutually avoiding; an initial configuration of the model is generated by a variant[36] of the Rosenbluth–Rosenbluth[42] technique. Of course, these initial configurations need not yet exhibit the proper statistical properties of the chains and therefore are carefully relaxed by a dynamic Monte–Carlo algorithm[34] allowing for motions of two and three adjacent bonds on the lattice[43] as well as end bond motions. For $\phi_v = 0.8$ and $\phi_v = 0.4$, only the case $N = 16$ is considered, while for $\phi_v = 0.6$ $N$ is varied from $N = 8$ to $N = 64$. For $\phi_v = 0.2$, $N$ was varied from $N = 4$ to $N = 32$ in our previous work.[35,36]

While in the limit $\phi_v \to 0$ it is a single energy parameter $\epsilon \equiv \epsilon_{AB} - (\epsilon_{AA} + \epsilon_{BB})/2$ which matters, cases with the same $\epsilon$ but different choices for $\epsilon_{AA}$, $\epsilon_{BB}$, and $\epsilon_{AB}$ are no longer equivalent for $\phi_v \neq 0$. We have therefore studied three choices of energy parameters: (1) $\epsilon_{AA} = \epsilon_{BB} = -\epsilon$, $\epsilon_{AB} = 0$; (2) $\epsilon_{AB} = \epsilon$, $\epsilon_{AA} = \epsilon_{BB} = 0$; (3) $\epsilon_{AA} = \epsilon_{BB} = -\epsilon_{AB} = -\epsilon/2$. Note that no energy parameters are included involving the solvent (or vacancies). These energy parameters are taken into account in the Monte Carlo sampling of configurations in the standard way[32–34] via the transition probability $w$. For each attempted move that is consistent with the excluded volume restrictions one computes the change in the number of nearest-neighbor AA, BB, and AB pairs and hence the resulting energy change $\Delta E$. The move is executed only if the transition probability $w \equiv \exp(-\Delta E/k_B T)$ exceeds a random number $\zeta$ that is uniformly distributed between zero and unity.

The main novel feature of our Monte Carlo algorithm[35,36] is the fact that the simulation is carried out in the grandcanonical ensemble of the mixture; i.e., the chemical potential difference $\Delta\mu$ between the A and B monomers is held fixed, rather than the relative concentration $\phi_A/(\phi_A + \phi_B) = \phi_A/(1 - \phi_v)$. This means that every $k$th step [where $k$ is typically between 1 (for $\Delta\mu = 0$) and 100, in units of Monte Carlo steps per bond; it has been checked that the results for the thermodynamic properties defined below (eq 4–8) do not depend on $k$] we consider an attempted move where the chain configuration is held fixed but the chain changes its identity. In the transition probability $w$, a term $\Delta\mu N$ (for a transition A → B) or $-\Delta\mu N$ (for a transition B → A) is then included in the energy change $\Delta E$. The number of configurational relaxation steps $k$ between these attempted chain relabelings must be large for $\phi_A$ very different from $\phi_B$, since we find the linear dimensions of the A chains to differ from those of the B chains in the general case where $\phi_A \neq \phi_B$, see Figure 1, even though we consider only cases with $\epsilon_{AA} = \epsilon_{BB}$. In the absence of these attractive interaction parameters ($\epsilon_{AA} = \epsilon_{BB} = \epsilon_{AB} = 0$) all chains have the same linear dimensions.

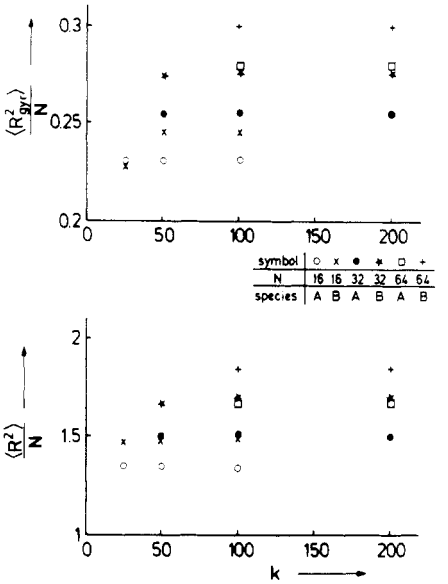


**Figure 1.** Plot of the mean-square gyration radius (upper part) and mean-square end-to-end distance (lower part), normalized per chain length $N$, versus the number $k$ of steps between the grandcanonical chain relabeling trials. These results have been recorded for $\phi_v = 0.6$, $\phi_A = 0.04$, $\phi_B = 0.36$. For all chain lengths the temperature $k_B T/\epsilon$ is chosen such that $m = (\phi_B - \phi_A)/0.4 = 0.8$ corresponds to the coexistence curve ($\Delta\mu = 0$). This calculation was performed choosing $\epsilon_{AB} = 0$.

The quantities calculated from the Monte Carlo sampling include the number of A and B chains in the system, $n_A$ and $n_B$, respectively, which immediately yields the "order parameter" $M$ of the unmixing transition of the mixture

$$M \equiv \Delta n/n \qquad n \equiv n_B + n_A, \quad \Delta n \equiv n_B - n_A \tag{4}$$

Since in a finite lattice $\langle M \rangle = 0$, the quantity recorded to calculate the coexistence curve is $m \equiv \langle |M| \rangle$. In our symmetrical model, the coexistence curve is then obtained as follows [$\phi_{crit} = (1 - \phi_v)/2$]:

$$\phi_{B,1}^{coex} = \phi_{crit}(1 - m) = \phi_{A,2}^{coex}$$

$$\phi_{B,2}^{coex} = \phi_{crit}(1 + m) = \phi_{A,1}^{coex} \tag{5}$$

From a sampling of the fluctuations of $M$, we obtain the maximum value $S_{coll}(k=0)$ of the collective structure factor $S_{coll}(\vec{k})$, namely[36]

$$S_{coll}(\vec{k}=0) = nN(1 - \phi_v)[\langle M^2 \rangle - \langle |M| \rangle^2] \tag{6}$$

with $S_{coll}(\vec{k})$ being defined as the Fourier transform of the fluctuations in the relative concentration $|\phi_B{}^j - \phi_A{}^j| - \langle|\phi_B{}^j - \phi_A{}^j|\rangle$

$$S_{coll}(\vec{k}) \equiv \langle[\sum_j \exp(i\vec{k}\cdot\vec{R}_j)(|\phi_B{}^j - \phi_A{}^j| - \langle|\phi_B{}^j - \phi_A{}^j|\rangle)]^2\rangle/L^3 \quad (7)$$

where the sum extends over all lattice sites $j$ and $\phi_A{}^j(\phi_B{}^j)$ is unity if site $j$ is taken by an A(B) atom and otherwise zero.

Furthermore, we obtain the average energy $\langle E\rangle$ in the system and the specific heat from the sampling of energy fluctuations

$$C_s = L^3(\langle E^2\rangle - \langle E\rangle^2)/k_BT^2 \quad (8)$$

Here $E$ is the internal energy normalized per lattice site; the specific heat $C_s$ is also normalized per lattice site.

Next, we consider the mean-square end-to-end distances $\langle R^2\rangle_A$ and $\langle R^2\rangle_B$ and the mean-square gyration radii $\langle R^2_{gyr}\rangle_A$ and $\langle R^2_{gyr}\rangle_B$ of the chains

$$\langle R^2\rangle_A = \langle\sum_{j=1}^{n_A}(\vec{r}_{jN} - \vec{r}_{j1})^2/n_A\rangle$$

$$\langle R^2\rangle_B = \langle\sum_{j=1}^{n_B}(\vec{r}_{jN} - \vec{r}_{j1})^2/n_B\rangle \quad (9)$$

$$\langle R^2_{gyr}\rangle_A = \langle\sum_{j=1}^{n_A}\sum_{k<l}(\vec{r}_{jl} - \vec{r}_{jk})^2/n_A\rangle/N^2$$

$$\langle R^2_{gyr}\rangle_B = \langle\sum_{j=1}^{n_B}\sum_{k<l}(\vec{r}_{jl} - \vec{r}_{jk})^2/n_B\rangle/B^2 \quad (10)$$

where $\vec{r}_{jk}$ is the site of the $k$th effective unit of the $j$th chain of species A or B, respectively.

Figures 2–4 now show some examples on the simulation results and their analysis. Figure 2a shows the order parameter as a function of temperature, for $\phi_v = 0.6$, $N = 64$, and $\Delta\mu = 0$. With eq 5 these results can be used to construct the coexistence curve of the model. While for $T \lesssim 0.9T_c$ the results are independent of the linear dimension $L$ of the box, and hence representative of the behavior in the thermodynamic limit, $L \to \infty$, pronounced finite-size effects are seen for $T \gtrsim 0.9T_c$. Of course, the finite-size "tails" of the order parameter $m(T,L) = \langle|M|\rangle_{T,L}$ for $T > T_c$ are effects due to fluctuations which must give nonzero contributions in finite systems. Such phenomena are well-known and well understood in the simulation study of other phase transitions in condensed matter physics too.[32,33] There exists a standard extrapolation procedure, based on the so-called "finite-size scaling theory",[39-41] see eq 12 and 13 and Figures 3 and 4 below, from which the asymptotic behavior of $m(T,L\to\infty)$, included as a broken curve in Figure 2, is obtained.

Similar size effects are seen in the structure factor $S_{coll}$ shown in Figure 2b. Since these data are taken for $\Delta\mu = 0$, they represent critical scattering where for $T > T_c$ one follows a path at constant critical concentration $\phi_A = \phi_B = \phi_{crit} = (1 - \phi_v)/2$, while for $T > T_c$ one would follow a path exactly along the coexistence curve in the $T - \phi_A$ diagram.

Extrapolation of the positions $T_{max}(L)$ where $S_{coll}$ has its peak [and similarly extrapolation of the positions where the specific heat $C_s$ (eq 8) has its peak, ref 35, 36] yields one criterion for the location of the critical temperature $T_c$ of the model. Of course, phase transitions in a strict sense can occur in the thermodynamic limit, $L \to \infty$, only, while for finite $L$ all quantities ($m$, $S_{coll}(0)$, $C_s$, etc.) must have a smooth variation with temperature, as obtained. Nevertheless, we can estimate the location of $T_c$ with reasonable accuracy (relative accuracy 1% or better); an-

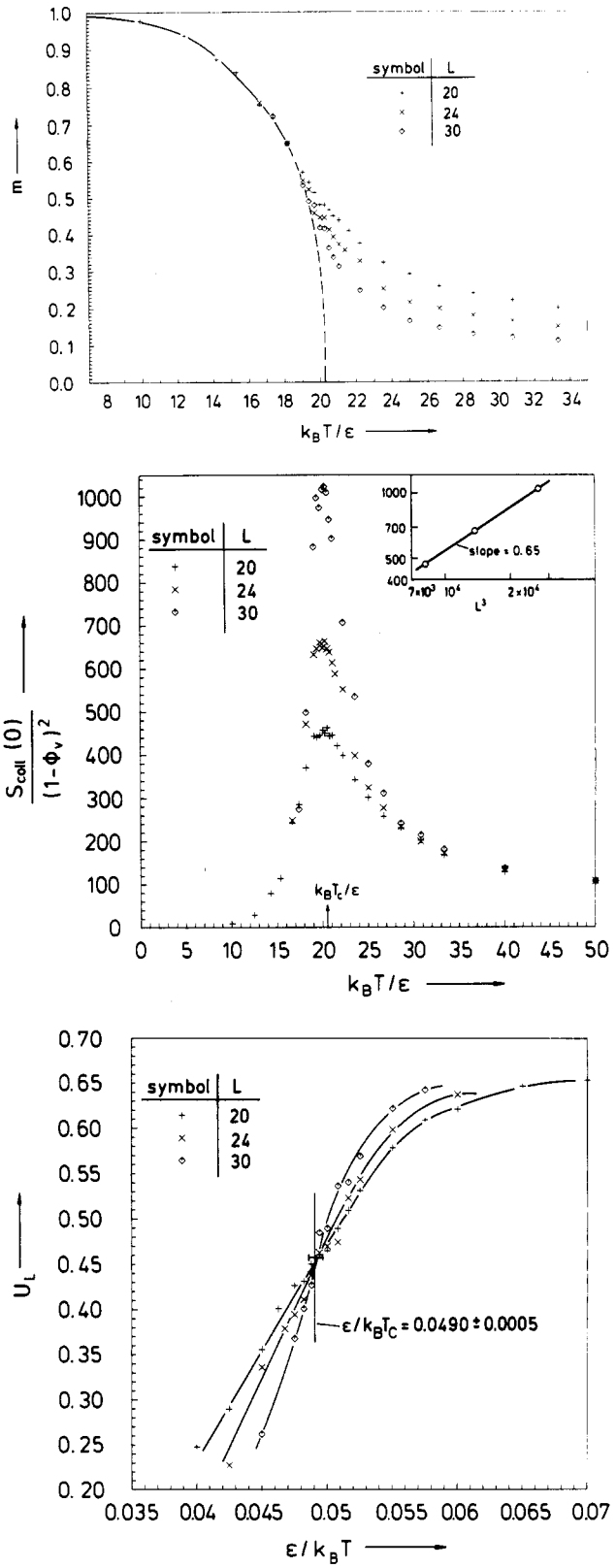


**Figure 2.** Order parameter $m$ plotted versus $k_BT/\epsilon$ (a, top), structure factor $S_{coll}(k=0)$ plotted versus $k_BT/\epsilon$ (b, middle), and cumulant $U_L$ plotted versus $\epsilon/k_BT$ (c, bottom). All results refer to the case $N = 64$, $\phi_v = 0.6$, $\Delta\mu = 0$, and $\epsilon_{AB} = 0$. Broken curve in case a is based on the finite-size scaling analysis, see Figure 3a, representing the law $m = \hat{B}(1 - T/T_c)^\beta$, with $\beta = 0.32$, $\hat{B} = 1.3$, $\epsilon/k_BT_c = 0.0490$. Three values of $L$ are shown as indicated in the figure. Insert of part b is a log–log plot of the maximum value of $S_{coll}(0)$ versus box volume.

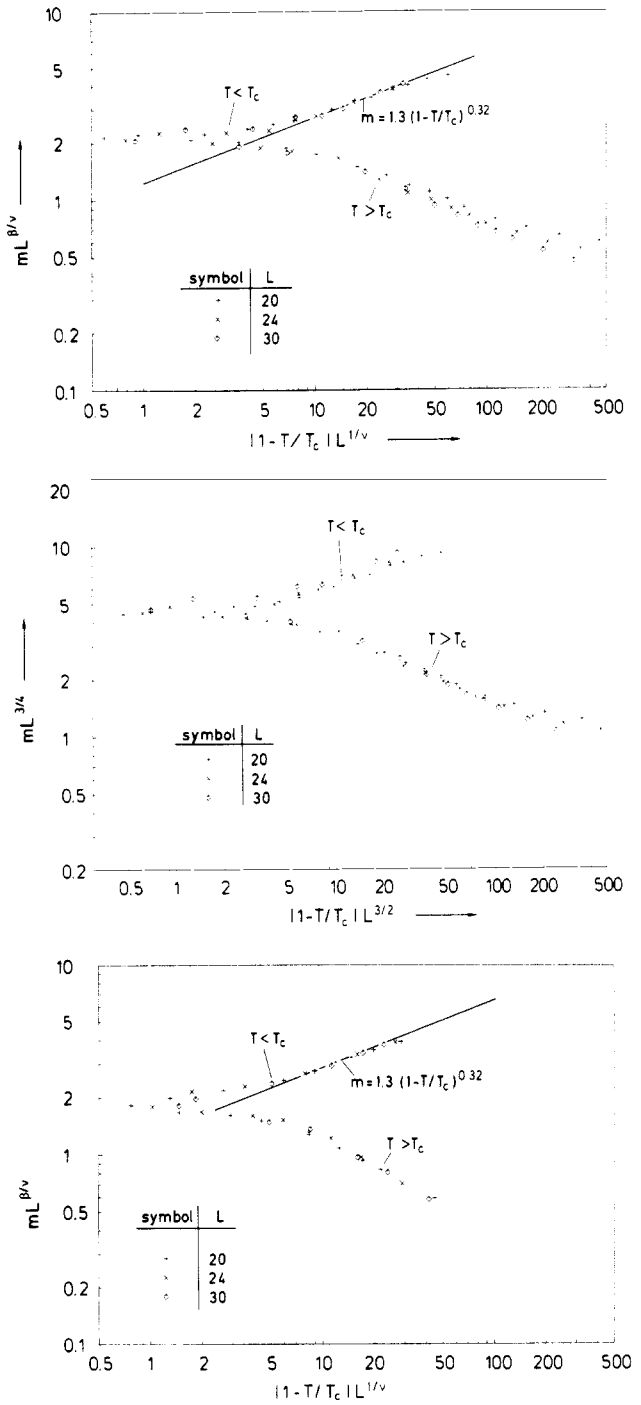


**Figure 3.** Finite-size scaling plots of the order parameter $mL^{\beta/\nu}$ plotted versus $|1 - T/T_c|L^{1/\nu}$ for the model with $\phi_v = 0.6$ and $\epsilon_{AB} = 0$. Case a (top) refers to $N = 64$ using Ising exponents ($\beta = 0.32$, $\nu = 0.63$) while case b (middle) also refers to $N = 64$ but uses the mean-field form of finite-size scaling, eq 15. Both cases a and b use $\epsilon/k_BT_c = 0.049$ as implied by Figure 2c. Case c (bottom) refers to $N = 16$, using $\epsilon/k_BT_c = 0.1661$ and the Ising exponents.

other independent criterion to locate $T_c$ is the intersection point of the cumulant $U_L$ defined as

$$U_L \equiv 1 - \langle M^4 \rangle / (3\langle M^2 \rangle^2) \tag{11}$$

if $U_L$ for several choices of $L$ is plotted vs temperature (Figure 2c). While the justification for getting $T_c$ from an extrapolation of $T_{max}(L)$ is obvious, the justification of the cumulant intersection method[40] really is due to finite-size scaling theory, which implies[39-41]

$$U_L(T) = \tilde{U}\{(1 - T/T_c)L^{1/\nu}\}$$
$$T \to T_c,\ L \to \infty,\ (1 - T/T_c)L^{1/\nu} \text{ finite} \tag{12}$$

where $\tilde{U}(\zeta)$ is a scaling function which behaves as $\tilde{U}(\zeta \to -\infty) \to 0$, $\tilde{U}(\zeta \to +\infty) = {}^2/_3$, while $\tilde{U}(0)$ is a nonzero positive constant. In eq 12, $\nu$ is the critical exponent[44] of the correlation length of the concentration fluctuations, $\xi \propto |1 - T/T_c|^{-\nu}$. Equation 12 simply expresses the fact that in the critical region $U_L(T)$ should be simply a function of the ratio $L/\xi$ but should not depend on these two lengths independently.[39] As a consequence, the curves $U_L(T)$ for different $L$ must intersect in a common intersection point $\tilde{U}(0)$ if $T = T_c$, and this fact is borne out by the Monte Carlo results (Figure 2c). Of course, there always is some scatter due to statistical errors,[32,33] and also for not too large $L$ (and temperatures not too close to $T_c$) there are also some systematic corrections to finite-size scaling, which holds in the limit specified in eq 12 only; but in spite of these practical limitations (which can be reduced, if necessary, by investing a considerably larger effort in computer time), we are able in practice to estimate $T_c$ with a relative accuracy of 1% or better for our model. As will be noted in section 3, this accuracy by far is good enough to provide a sensitive test for the Flory–Huggins approximation and related theories.

Another consequence of finite-size scaling is that the family of curves $m(T,L)$ in Figure 2a can be collapsed on a scaling function $\tilde{m}\{\zeta\}$ by rescaling the variables $m$ and $(1 - T)/T_c$ as follows:[39,40]

$$mL^{\beta/\nu} = \tilde{m}\{(1 - T/T_c)L^{1/\nu}\} \qquad T \to T_c,\ L \to \infty \tag{13}$$

where $\beta$ is the exponent of the order parameter in the asymptotic power law, which applies in the thermodynamic limit

$$m(T,L\to\infty) = \hat{B}(1 - T/T_c)^{\beta} \qquad T \to T_c \tag{14}$$

with $\hat{B}$ being the "critical amplitude".[44] Since a careful analysis of our results for $\phi_v = 0.2$ has revealed that the critical behavior for $N \leq 32$ is still fully consistent with the exponents of the "Ising universality class",[44] namely,[45] $\beta \cong 0.32$, $\nu \cong 0.63$, $\gamma \cong 1.24$, we use these Ising exponents also in the present case, Figures 3 and 4. Although it is predicted[17,29,46] that for $N \to \infty$ one should rather observe mean-field exponents,[44] $\beta = {}^1/_2$, $\gamma = 1$, $\nu = {}^1/_2$, there is no evidence for a mean-field critical regime even for chains as long as $N = 64$: the peak value of the structure factor $S_{coll}^{max}$ behaves as $S_{coll}^{max} \propto L^{\gamma/\nu} = (L^3)^{0.65}$, see insert of Figure 2b, as finite-size scaling using Ising exponents implies.[39] In contrast, the mean-field version of finite-size scaling would require[41] $S_{coll}^{max} \propto L^{3/2}$ for $d = 3$ dimensions; such a law is not consistent with our results. When in the finite-size scaling of the order parameter instead of eq 13 the mean-field formula[41]

$$mL^{3/4} = \tilde{m}\{(1 - T/T_c)L^{3/2}\} \qquad T \to T_c,\ L \to \infty \tag{15}$$

is used, where $\tilde{m}\{\zeta\}$ is another scaling function, significantly worse "data collapsing" is obtained (Figure 3b).

Just as has been illustrated here for the case $N = 64$, $\phi_v = 0.6$, we have proceeded for all other values of $N$ and $\phi_v$ studied, too, as well as in the case where $\epsilon_{AB}$ is nonzero. It turns out that the results always are qualitatively rather similar to each other, and hence only a small sample of our results is shown in Figure 4. In all cases studied we obtain a reasonable fit of the critical behavior with Ising exponents, the order parameter amplitude $B \approx 1.3 \pm 0.1$ being independent of both $N$ and $\phi_v$, within our error limits. However, an interesting systematics seems to emerge with respect to the dependence of $T_c$ on both $N$ and $\phi_v$, as will be discussed in the next section.

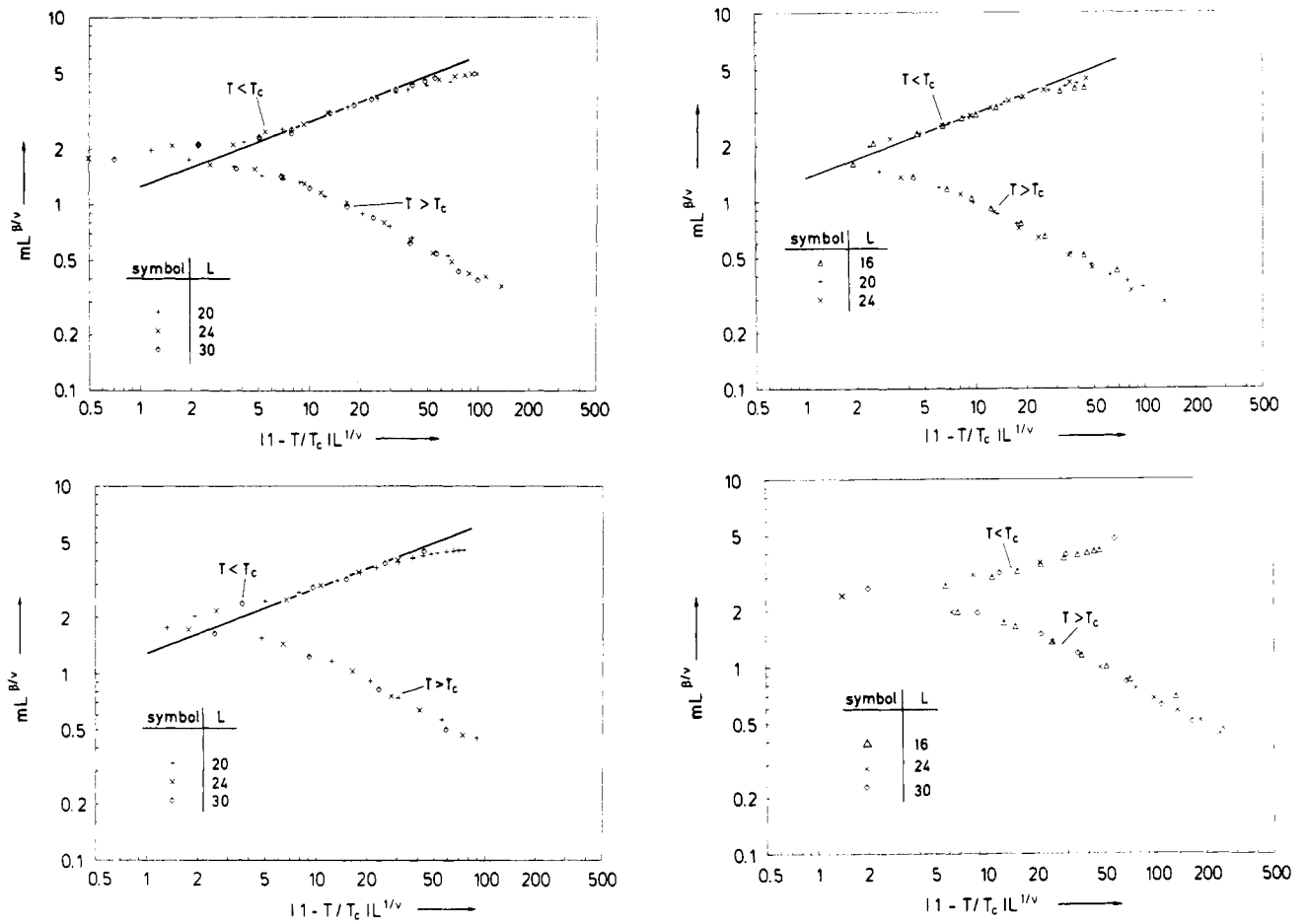


**Figure 4.** Finite-size scaling plots of the order parameter, $mL^{\beta/\nu}$ plotted versus $|1 - T/T_c|L^{1/\nu}$, $T/T_c|L^{1/\nu}$, for a variety of cases. Ising exponents ($\beta = 0.32$, $\nu = 0.63$) are used throughout. Case a (top left) refers to the choice $N = 16$, $\phi_v = 0.6$, $\epsilon_{AA} = \epsilon_{AB} = 0$, using $\epsilon/k_BT_c = 0.1881$. Case b (bottom left) refers to the choice $N = 16$, $\phi_v = 0.6$, $\epsilon_{AA} = \epsilon_{BB} = -\epsilon_{AB}$, using $\epsilon/k_BT_c = 0.177$. Case c (top right) refers to the choice $N = 16$, $\phi_v = 0.4$, $\epsilon_{AB} = 0$, using $\epsilon/k_BT_c = 0.0921$. Case d (bottom right) refers to the choice $N = 16$, $\phi_v = 0.8$, $\epsilon_{AA} = \epsilon_{BB} = -\epsilon_{AB}$, using $\epsilon/k_BT_c = 0.52$. Straight lines always show the asymptotic law $m = \hat{B}(1 - T/T_c)^\beta$ with $\beta = 0.32$, $\hat{B} = 1.3$.

## 3. Equation of State of the Flory–Huggins Model and Comparison to Theoretical Predictions

First we recall the explicit predictions resulting from the Flory[1] and Guggenheim[12] approximations for the equation of state of our symmetrical Flory–Huggins lattice model ($N_A = N_B = N$) in the limit of zero vacancy concentration ($\phi_v = 0$). It is convenient to start from the following expressions for the chemical potential difference $\Delta\mu_A$ and $\Delta\mu_B$, normalized per chain, in the Guggenheim[12] approximation[47]

$$\frac{\Delta\mu_A}{k_BT} = \ln \phi_A + \frac{1}{2}zq \ln \frac{1 - K\phi_B}{\phi_A} \tag{16a}$$

$$\frac{\Delta\mu_B}{k_BT} = \ln \phi_B + \frac{1}{2}zq \ln \frac{1 - K\phi_A}{\phi_B} \tag{16b}$$

where $q \equiv N(1 - 2/z) + 2/z$ and $K$ is related to the energy parameter $\epsilon$ via

$$(1 - K) = K^2\phi_A\phi_B(e^{2\epsilon/k_BT} - 1) \tag{17}$$

In eq 16, $\Delta\mu_A$ ($\Delta\mu_B$) denotes the change in free enthalpy (Gibbs free energy) when an A chain (or B chain, respectively) is added to the system. The chemical potential difference $\Delta\mu$ between an A segment and a B segment on a lattice site (this is the quantity thermodynamically conjugate to the relative segment concentration $\phi = \phi_A/(\phi_A + \phi_B) = \phi_A$) thus becomes

$$\frac{\Delta\mu}{k_BT} = \frac{1}{N}\left(\frac{1}{2}zq - 1\right) \ln \frac{\phi_B}{\phi_A} - \frac{1}{2N}zq \ln \frac{1 - K\phi_A}{1 - K\phi_B} \tag{18}$$

where the appropriate solution of the quadratic equation 17 for $K$ is

$$K = \frac{1}{2\phi_A\phi_B(e^{2\epsilon/k_BT} - 1)}\{(1 + 4\phi_A\phi_B(e^{2\epsilon/k_BT} - 1))^{1/2} - 1\} \tag{19}$$

From eq 18 and 19 the Flory approximation results from the two following approximations: (1) Since for the temperature regime of interest, $\epsilon/k_BT \ll 1$, one may replace $e^{-2\epsilon/k_BT} - 1$ by $-2\epsilon/k_BT$ and expand the square root to obtain

$$K \approx 1 - \phi_A\phi_B\frac{2\epsilon}{k_BT} \tag{20}$$

and also expand $\ln (1 - K\phi_A)/(1 - K\phi_B)$ to first order in $\epsilon/k_BT$ to obtain

$$\frac{\Delta\mu}{k_BT} \cong \frac{1}{N} \ln \frac{\phi_A}{\phi_B} + \frac{zq\epsilon}{Nk_BT}(\phi_B - \phi_A) \tag{21}$$

(2) The factor $q/N$ is replaced by unity, which obviously is correct for $z \to \infty$ only. With these approximations, eq 21 coincides with the result found from eq 2 and 3 for $N_A = N_B = N$, remembering $\Delta\mu/k_BT \equiv \partial(\Delta G/k_BT)/\partial\phi$, $\phi_B = 1 - \phi$, $\phi_A = \phi$. From eq 21 we then obtain the inverse of the collective structure function as the second derivative

$$S^{-1}_{coll}(q=0) = [\partial(\Delta\mu/k_BT)/\partial\phi] = \frac{1}{N\phi_A\phi_B} - 2\chi \tag{22}$$

Equation 22 yields the prediction for the critical point occurring at $\phi_A = \phi_B = {}^1/_2$ and $\chi_{AB} = \chi_c = 2/N$.

We now wish to obtain $S^{-1}_{coll}(q=0)$ from the more accurate eq 18. This yields

$$S^{-1}_{coll}(q=0) = \frac{1}{N\phi_A\phi_B}\left(1 - \frac{1}{2}zq\right) + \frac{zq}{2N}\left\{\frac{(w-1)/[2\phi_B{}^2(e^{2\epsilon/k_BT}-1)] + (\phi_B - \phi_A)/(\phi_B w)}{1-(w-1)/[2\phi_B(e^{2\epsilon/k_BT}-1)]} + \frac{(w-1)/[2\phi_A{}^2(e^{2\epsilon/k_BT}-1)] - (\phi_B-\phi_A)/(\phi_A w)}{1-(w-1)/[2\phi_A(e^{2\epsilon/k_BT}-1)]}\right\} \quad (23)$$

where we have introduced the abbreviation $w = [1 + 4\phi_A\phi_B(e^{2\epsilon/k_BT} - 1)]^{1/2}$. The critical point still occurs for $\phi_A = \phi_B = {}^1/_2$, which yields $w = e^{\epsilon/k_BT}$ and hence

$$S^{-1}_{coll}(q=0) = \frac{4}{N} - \frac{2zq}{N} + \frac{2zq}{N}e^{\epsilon/k_BT} \quad (24)$$

from which one finds the critical temperature in the Guggenheim approximation as[12]

$$\frac{\epsilon}{k_BT_c} = -\ln\left(1 - \frac{2}{zq}\right) = -\ln\left[1 - \frac{2}{N(z-2)+2}\right] \approx \frac{2}{N(z-2)+2} \quad (25)$$

The Flory approximation again follows for $z \to \infty$, i.e., $(z\epsilon/k_BT_c)_{Flory} = 2/N$. From eq 17 and 18 we obtain for $\Delta\mu = 0$ the equation of the coexistence curve (binodal) as [$\phi_A = (1+m)/2$; $\phi_B = (1-m)/2$]

$$\ln\frac{1-m}{1+m} = \frac{zq}{2}\ln\frac{1 + ((1-m)/(1+m))(1-K)}{1 + ((1+m)/(1-m))(1-K)} \quad (26a)$$

with

$$2\epsilon/k_BT = \ln\left[1 + 4\frac{1-K}{K^2(1-m^2)}\right] \quad (26b)$$

Solving eq 26a for $K = K(m)$ allows a straightforward evaluation of the inverse function of the coexistence curve, i.e., $\epsilon/k_BT$ as a function of $m$.

From eq 26 we also can find the Flory approximation using eq 20 and expanding the logarithm on the right-hand side of eq 26a to find

$$\ln\frac{1-m}{1+m} = -zq\frac{\epsilon}{k_BT}m = -N\chi m \quad (27)$$

To our knowledge, the Guggenheim[12] approximation has not yet been worked out in detail for ternary systems. The Flory[11] approximation, on the other hand, is straightforwardly extended[48] to the present ternary system with $N_A = N_B = N$. Equation 3 is replaced by

$$\frac{\Delta G}{k_BT} = \frac{\phi_A\ln\phi_A + \phi_B\ln\phi_B}{N} + \phi_v\ln\phi_v + \chi_{AB}\phi_A\phi_B + \frac{1}{2}\chi_{AA}\phi_A{}^2 + \frac{1}{2}\chi_{BB}\phi_B{}^2 \quad (28)$$

Writing now

$$\phi_A = [(1-\phi_v)(1+m)]/2 \qquad \phi_B = [(1-\phi_v)(1-m)]/2 \quad (29)$$

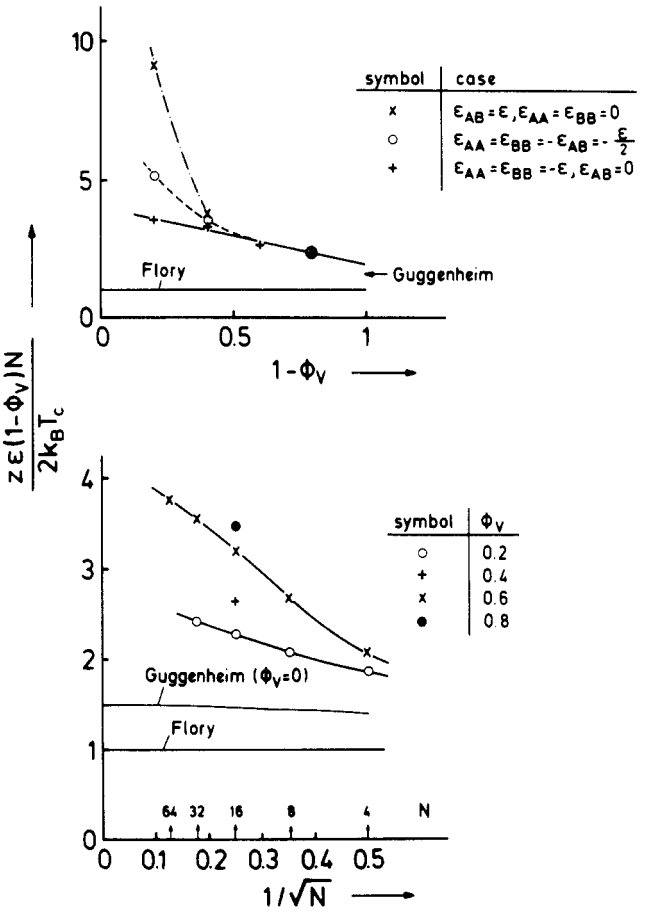


**Figure 5.** Inverse critical temperature plotted versus the polymer concentration (upper part) and versus the inverse of the square root of the chain length (lower part). Always the normalization is chosen in units of the Flory prediction for the inverse critical temperature. Upper part refers to $N = 16$. Curves are only drawn to guide the eye. Note that in the upper part for $1 - \phi_v = 0.8$ all three cases yield the same value of $T_c$ (solid dot).

one finds for the part $\Delta G'$ of the Gibbs free energy that depends on $m$

$$\frac{\Delta G'}{k_BT(1-\phi_v)} \equiv \frac{\Delta G - \phi_v\ln\phi_v}{k_BT(1-\phi_v)} - \frac{1}{N}\ln(1-\phi_v) - \frac{1-\phi_v}{8}(\chi_{AA} + 2\chi_{AB} + \chi_{BB}) = \frac{1}{N}\left\{\frac{1+m}{2}\ln\left(\frac{1+m}{2}\right) + \frac{1-m}{2}\ln\left(\frac{1-m}{2}\right)\right\} + \frac{(1-\phi_v)(\chi_{AA}-\chi_{BB})}{4}m + \frac{1-\phi_v}{8}(\chi_{AA} + \chi_{BB} - 2\chi_{AB})m^2 \quad (30)$$

It is seen that $\Delta G'(\phi_v)/(1-\phi_v)$ has the same structure that $\Delta G'(\phi_v = 0)$ has if we introduce the renormalized Flory parameters

$$\tilde{\chi}_{AA} = (1-\phi_v)\chi_{AA} \qquad \tilde{\chi}_{AB} = (1-\phi_v)\chi_{AB} \qquad \tilde{\chi}_{BB} = (1-\phi_v)\chi_{BB} \quad (31)$$

In particular, we obtain the condition for the critical point now as[36,48]

$$\chi_c \equiv \chi_{AB} - {}^1/_2[(\chi_{AA} + \chi_{BB})]_{T=T_c} = 2/[(1-\phi_v)N] \quad (32a)$$

where in our notation

$$\chi_{AB} = z\epsilon_{AB}/k_BT \qquad \chi_{AA} = z\epsilon_{AA}/k_BT \qquad \chi_{BB} = z\epsilon_{BB}/k_BT \quad (32b)$$

In Figure 5 we are now comparing eq 32a and 25 to our numerical results. From this comparison the following conclusions immediately emerge: (1) In all cases the Flory approximation overestimates the critical temperature by at least a factor of 2. The Guggenheim approximation (so far available for $\phi_v = 0$ only, where no computer simulation results exist) is distinctly better, but also not exact. (2) The Flory prediction, that adding vacancies produces a decrease in critical temperature according to a factor $1 - \phi_v$, also is a severe underestimate of the actual decrease of the critical temperature. (3) The Flory prediction, that it is only the combination $2\epsilon_{AB} - \epsilon_{AA} - \epsilon_{BB}$ (cf. eq 2 and 32) that matters for the location of the critical temperature, is rather accurate for $\phi_v \lesssim 0.5$ but breaks down completely for large vacancy concentration. Already for $\phi_v = 0.8$ critical temperatures for the three different cases studied in Figure 5 differ among themselves by up to a factor of 3!

We now proceed to compare our data for the full coexistence curve at $\phi_v = 0.6$ (Figure 6a) to the predictions of the Flory approximation (Figure 6b) and the Guggenheim approximation (Figure 6c). It is seen that the true shape of the coexistence curve near $T_c$ is much flatter than the Flory prediction. This reflects the non-mean-field value of the critical exponent $\beta$ in eq 14, $\beta \cong 0.32$, while the Flory result following from eq 27 simply is

$$m_{\text{Flory}} = \sqrt{3}(1 - T/T_c)^{1/2} \qquad T \to T_c \qquad (33a)$$

From the Guggenheim approximation, eq 26, one similarly derives

$$m_{\text{Gugg}} = \sqrt{3}(1 - T/T_c)^{1/2}\left(\frac{(1 - 2/zq)(\epsilon/k_BT_c)}{2/zq[1 - 3/zq + (2/zq)^2]}\right)^{1/2} \qquad (33b)$$

Since for very long chains $\epsilon/k_BT_c \approx 2/zq \to 0$, the critical amplitude for $m$ then takes the same value, $\sqrt{3}$, in both the Flory and the Guggenheim approximations. Thus although the Guggenheim approximation yields a flatter shape of the coexistence curve, it still yields mean-field critical behavior, as expected. The very pronounced deviation from mean-field critical behavior as found in the present work should occur for real polymer systems as well, due to the "universality principle" of critical phenomena.[44,45] But if the lattice coordination number (or the interaction range, respectively) increases, the range of temperatures where this non-mean-field Ising critical behavior occurs gets smaller. Similarly, a reduction of the Ising critical regime is expected to occur for large chain molecular weight, as discussed in ref 17, 29, and 36. At low temperatures, where $m \to 1$, both the Flory and the Guggenheim approximations yield the expression

$$m \cong 1 - 2\exp\left(-\frac{zq\epsilon}{k_BT}\right) \qquad (33c)$$

In the Flory approximation, however, $zq$ is replaced simply by $N$ in eq 33c.

Figure 7 shows the equation of state as obtained in our simulation for both $\phi_v = 0.2$ and $\phi_v = 0.6$. From these data we can define an "effective" Flory parameter $\chi$ by using eq 21

$$N\chi_{\text{eff}} \equiv \frac{1}{m}\left\{\ln\frac{1+m}{1-m} - \frac{N\Delta\mu}{k_BT}\right\} \qquad (34)$$

If the Flory theory were exact for the present model, we simply would have $(1 - \phi_v)\chi_{\text{eff}} = z\epsilon/k_BT$. Figure 8 shows the curves $\chi_{\text{eff}}(\phi_A,T)/[z(1 - \phi_v)]$ in the plane of variables $\epsilon/k_BT$ and $\phi_A$; instead of straight horizontal lines (equal to $\epsilon/k_BT$) we observe curves which throughout have a much smaller value. The curvature is the more pronounced the lower the temperature, while in the limit $\epsilon/k_BT \to 0$ $\chi_{\text{eff}}/[z(1 - \phi_v)]$ differs from $\epsilon/k_BT$ simply by a constant factor. In this limit, this factor just reflects the fact that the number of contacts that a monomer of one chain has with monomers of *other* chains is not $z(1 - \phi_v)$ but distinctly smaller. (Only the interaction of monomers of one chain with monomers of other chains can lead to

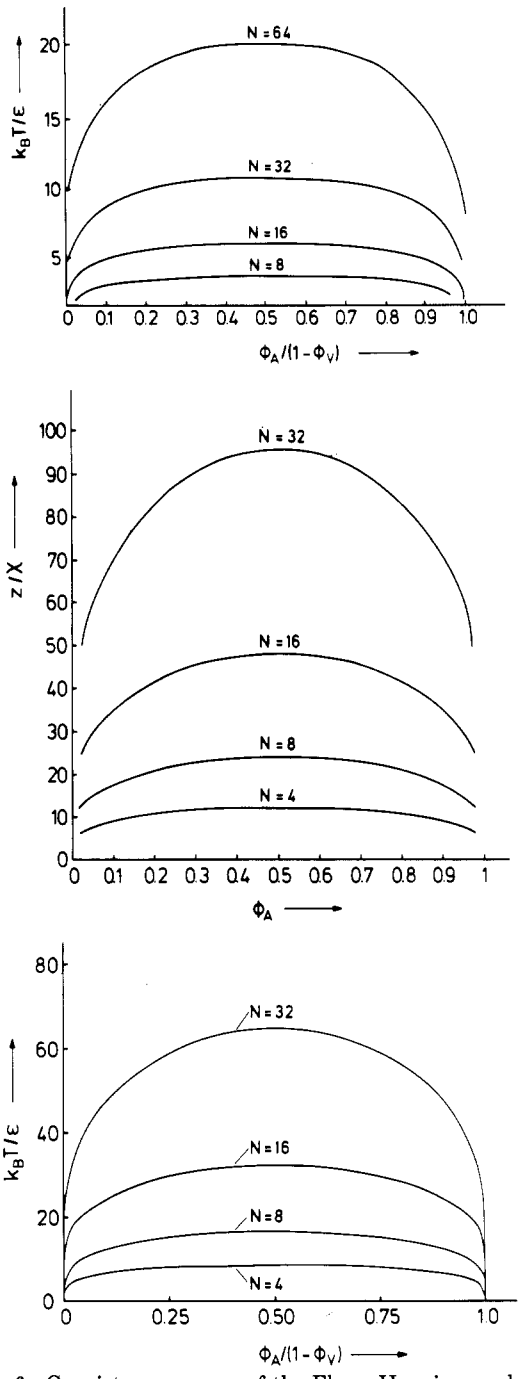


**Figure 6.** Coexistence curves of the Flory–Huggins model for several values of $N$ according to the Monte Carlo calculation for $\phi_v = 0.6$ (case a, top) compared to the coexistence curves as obtained from the Flory approximation, eq 27 (case b, middle), and the Guggenheim approximation, eq 26a,b (case c, bottom). Note that both case b and case c refer to $\phi_v = 0$, but case b is generalized to $\phi_v \neq 0$ simply by replacing $\chi$ by $\chi(1 - \phi_v)$ in this figure and $\phi_A$ by $\phi_A/(1 - \phi_v)$ as in case a.

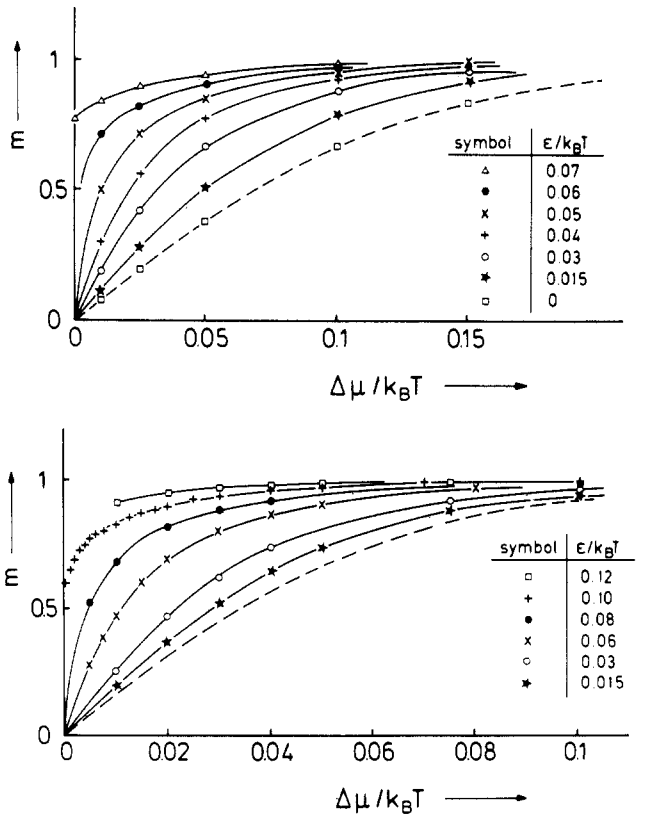


**Figure 7.** Plot of the order parameter $m$ $(=(\phi_A - \phi_B)/(1 - \phi_v))$ plotted versus the chemical potential difference $\Delta\mu/k_BT$ for several choices of $\epsilon/k_BT$, as indicated in the figure using $\phi_v = 0.2$ and $N = 16$ for case a (top) and $\phi_v = 0.6$ and $N = 32$ for case b (bottom). Full curves are guides to the eye only; broken curve is the limiting function resulting in the noninteracting case $(\epsilon/k_BT = 0)$, $m = \tanh[N\Delta\mu/(2k_BT)]$.

the phase separation considered here.) Although qualitatively this effect is accounted for in the Guggenheim approximation, where this number of contacts is taken to be $[(z - 2) + 2/N](1 - \phi_v)$, it is still significantly overestimated.

We can check this fact by applying the Guggenheim relation between $\Delta\mu$ and $m$, eq 18; from each point in Figure 7 and eq 18 we hence can extract an effective interaction parameter $\epsilon_{eff}$ as the effective Flory–Huggins parameter $\epsilon_{eff}(\phi_A,T)$ normalized by the factor $z(1 - \phi_v)$; Figure 9 shows that $\epsilon_{eff}/k_BT \equiv \epsilon_{eff}(\phi_A,T)/[z(1 - \phi_v)]$ is still significantly different from $\epsilon/k_BT$, although the discrepancies now are somewhat smaller than when the Flory approximation is used.

From Figure 7 it is seen that the equation of state in the noninteracting limit $\epsilon/k_BT \to 0$ is simply given by

$$m = \tanh(N\Delta\mu/2k_BT) \tag{35}$$

consistent with both the Flory and the Guggenheim approximations, which become identical in this limit. The error of both approximations is due to a wrong count of the number of contacts that a monomer of one chain makes with monomers of the other chains. This fact is illustrated more closely in Figure 10, where we plot for $\Delta\mu/k_BT = 0$ the number of contacts between monomers of different kind (AB) as a function of temperature, as well as the number of contacts (AA, BB) of the same kind, distinguishing between intrachain and interchain contacts. If correlations in the occupation of sites by vacancies as well as intrachain contacts were negligible, the sum of the AB contacts and the AA (or BB) intrachain contacts should be temperature-independent and given by the value $(1 - \phi_v)[N(z - 2) + 2]$. Figure 10 demonstrates that the actual

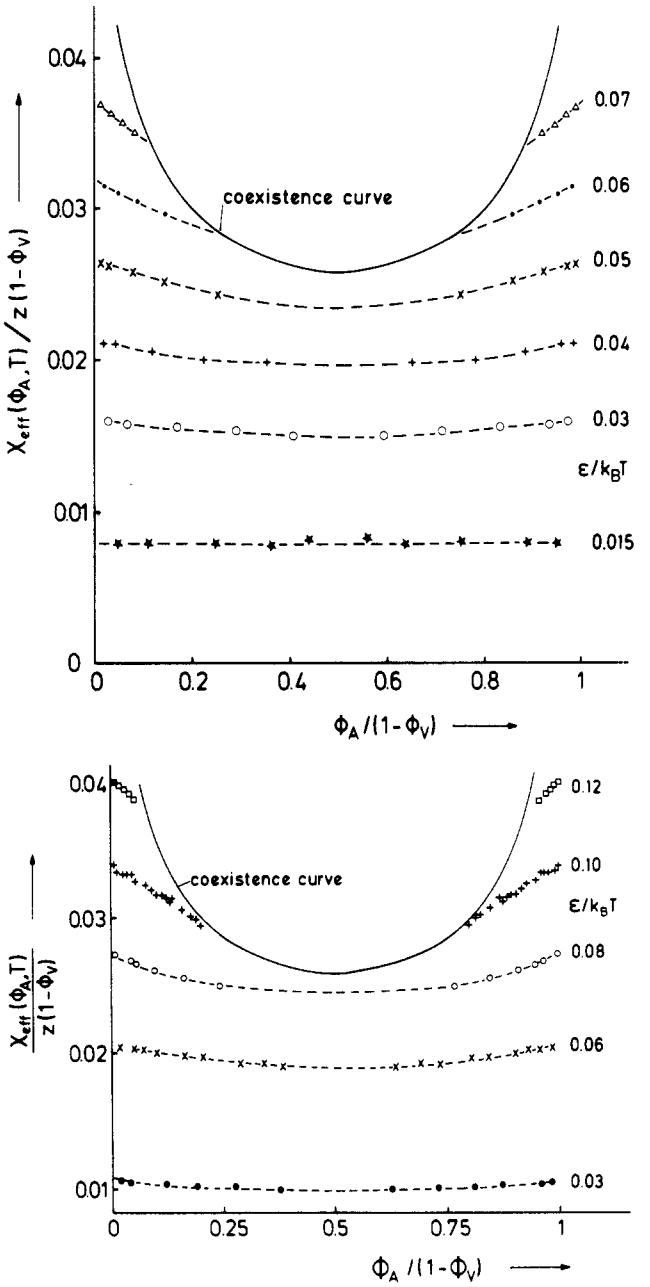


**Figure 8.** Plot of the effective interaction parameter $\chi_{eff}(\phi_A,T)/[z(1 - \phi_v)]$ versus $\phi_A/(1 - \phi_v)$ for several temperatures, using the data shown in Figure 7 and eq 34 (the Flory approximation): $\phi_v = 0.2$, $N = 16$ (a, top); $\phi_v = 0.6$, $N = 32$ (b, bottom). Broken curves are guides to the eye only.

number of this sum is indeed nearly temperature-independent, at least for $1 - \phi_v \geq 0.4$, but significantly smaller than the value quoted above. Even if one added the intrachain contacts (which then need to be counted twice), one would not yet quite reach this value; this fact indicates that correlations in the occupation of sites by vacancies are not completely negligible, in spite of the large value of $k_BT_c/\epsilon$ due to the large chain lengths in our model. The rather large number of intrachain contacts is probably mostly due to "crankshaft" configurations of three successive bonds. We can estimate the probability of these configurations in the approximation where the chains are treated as nonreversal random walks (NRRW). Then each bond has $z - 1$ orientations relative to the orientation of the previous bond, $z - 2$ orientations form a 90° angle on the simple cubic lattice, and the remaining orientation continues straight on. Only one out of the $z - 1$ orientations of the third bond leads to the crankshaft configu-

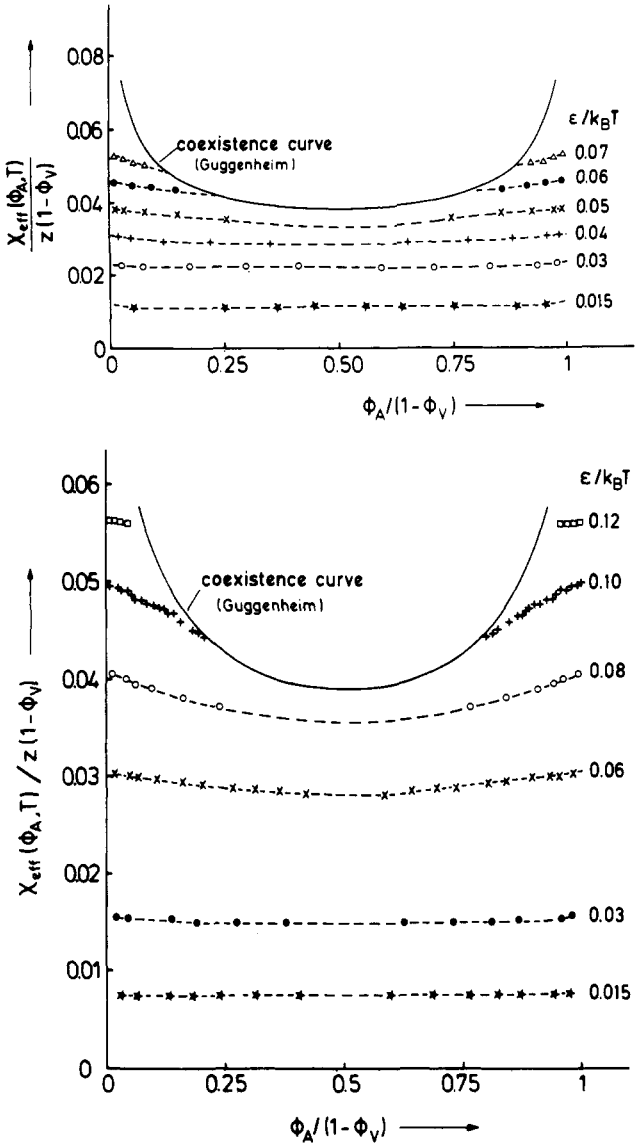


**Figure 9.** Plot of the effective interaction parameter $\chi_{eff}(\phi_A,T)/[z(1-\phi_v)]$ versus $\phi_A/(1-\phi_v)$ for several temperatures, using the data shown in Figure 7 and eq 18 (the Guggenheim approximation): $\phi_v = 0.2$, $N = 16$ (a, top); $\phi_v = 0.6$, $N = 32$ (b, bottom). Broken curves are guides to the eye only.

ration, and hence the probability is $(z-2)/(z-1)^2$. We can apply this argument in a chain with $N$ beads ($N-1$ bonds) for the first $N-3$ bonds independently and hence arrive at the estimate

$$n_c(\text{intrachain,crankshaft}) \approx [(N-3)(z-2)]/(z-1)^2 \tag{36}$$

which implies that for $N \to \infty$ the effective coordination number for interchain contacts only is $(z-2-2(z-2))/(z-1)^2$. A comparison of eq 36 to Figure 10 reveals that eq 36 actually is an underestimate, as expected; also, larger loops involving more than three successive bonds will lead to nearest-neighbor contacts, and thus eq 36 accounts only for about one-half of the actual intrachain contacts. Parts e and f of Figure 10 show that for high vacancy concentration and relatively low temperatures there is also a tendency of the chains to decrease their energy by forming more contacts at low temperature than at high temperature. Thus, we then expect a change of chain linear dimensions with temperature as well, as will be analyzed in the next section.

Often the usefulness of the Flory–Huggins theory is implied by its application to the analysis of scattering data for $S_{coll}(q)$. For example, a standard procedure is to plot $S^{-1}_{coll}(q=0)$ versus temperature, assuming that in the temperature regime of interest $\chi$ varies linearly with temperature. Then the linear extrapolation of $S^{-1}_{coll}(q=0)$ to the temperature where $S^{-1}_{coll}(q=0) = 0$ yields the critical temperature (if one works at the critical concentration) or a spinodal temperature (if one works at an off-critical concentration).

In Figure 11 we show that a related procedure would work even with our data. Of course, for our model $\chi$ is not expected to be linearly proportional to temperature over a wide temperature range; rather, one expects $\chi$ to vary linearly proportional with the inverse temperature (eq 2). Since (cf. eq 22 and 32a) $S^{-1}_{coll}(q=0) = 2(\chi_c - \chi)$ if we work at critical concentration, the quantity $(k_BT/\epsilon)S^{-1}_{coll}(q=0)$ is predicted to behave with temperature according to a simple straight line

$$\frac{k_BT}{\epsilon}S^{-1}_{coll}(0) = \frac{4}{(1-\phi_v)N}\frac{k_BT}{\epsilon} - 2z \tag{37}$$

and indeed plotting our "data" in this way one obtains curves strongly resembling straight lines (Figure 11). However, the intercept of these straight lines with the abscissa is not the theoretical number $(N(1-\phi_v)z/2 = 1.2N$ in the case displayed in Figure 11) but occurs at a much lower temperature.

In the regime between the effective mean-field critical temperature defined by the linear extrapolation in Figure 11 and the actual critical behavior, the inverse scattering intensity exhibits distinct curvature. This curvature is expected, because our model exhibits Ising-like critical behavior

$$S^{-1}_{coll}(0) \propto (T/T_c - 1)^{\gamma} \qquad \gamma \approx 1.24 \tag{38}$$

as discussed already in section 2. In real polymer systems (where the chain lengths considered typically are much larger) one expects such a crossover from a linear extrapolation to Ising critical behavior, if one studies mixtures close enough to their critical point. Very recently experimental evidence for such a crossover has in fact been given.[49]

## 4. Chain Linear Dimensions

In this section we are concerned with the examination of one of the basic ingredients of the Flory–Huggins and Guggenheim theories, namely, the assumption that the chain linear dimensions are essentially "ideal", described by Gaussian random walk statistics. Even though there is no doubt that in dense polymer systems the asymptotic properties of very long chains are described by Gaussian statistics,[1,28] this does not exclude that the prefactor in the relation $\langle R^2_{gyr}\rangle \propto N$ does depend on vacancy concentration $\phi_v$, temperature, and the relative concentration $\phi_A/(1-\phi_v)$ of the polymer species. For the simple cubic lattice model of dense polymer solutions, where one kind of chains is put on the lattice, the dependence of chain configurations on the vacancy concentration has already been studied extensively.[50-54] In figure 12 we present our results for $\langle R^2\rangle$ and $\langle R^2_{gyr}\rangle$ for temperatures $T \to \infty$, i.e., the noninteracting case; in this limit our results become independent of the relative concentration $\phi_A/(1-\phi_v)$, since then there is no longer any distinction between the properties of A chains and B chains. Thus, this limit reduces to the problem studied in previous work,[50-54] and as Figure 12 demonstrates, our data are in very good agreement with these previous calculations. In Figure 12 we also include the predictions obtained if the self-avoiding walk restriction

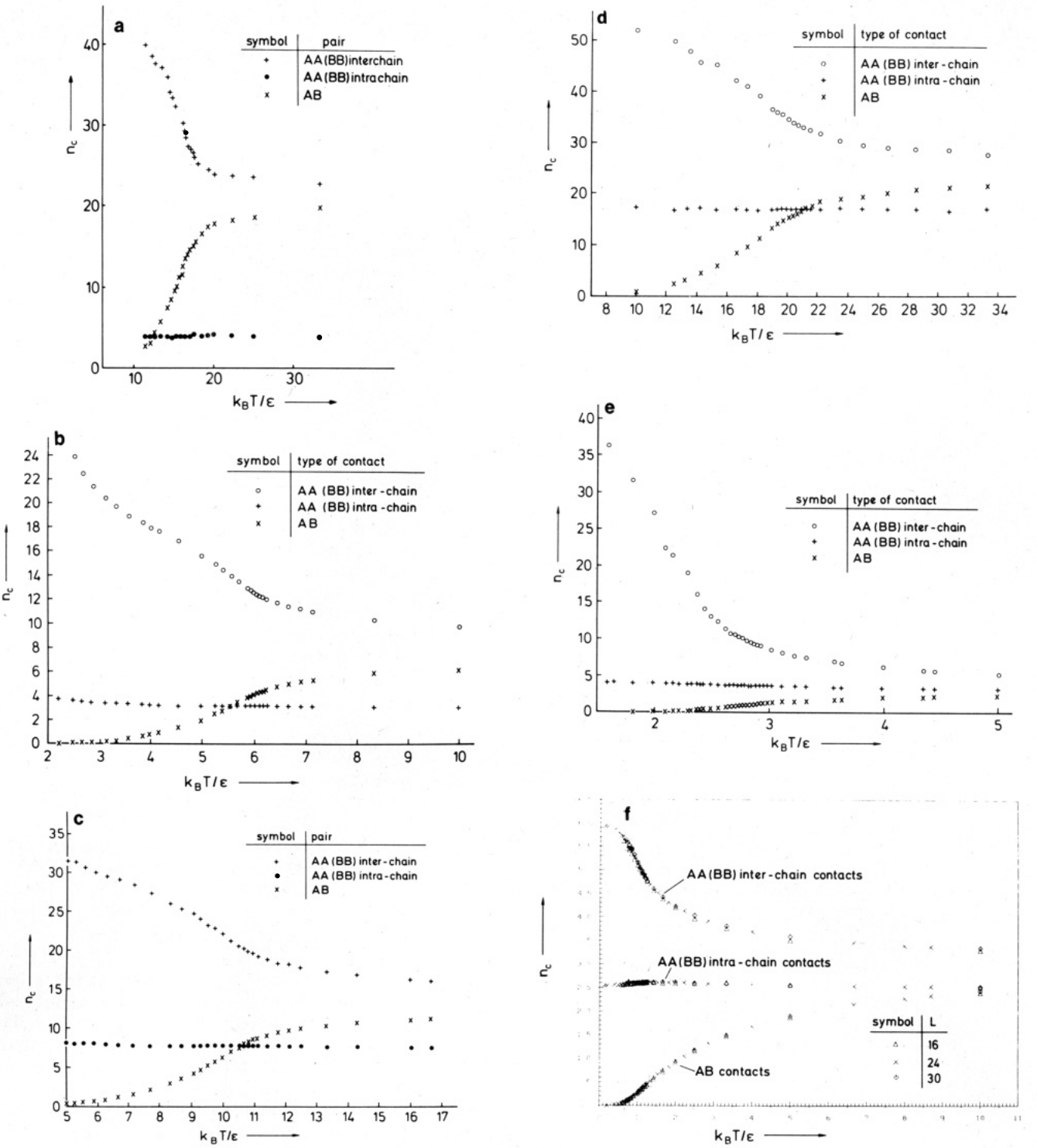


**Figure 10.** Plot of the number of contacts $n_c$ versus temperature, distinguishing contacts between monomers of different kind (AB), between interchain contacts of the same kind (AA, BB), and between intrachain contacts. Various cases are shown: (a) $N = 16$, $\phi_v = 0.2$, $\epsilon_{AB} = 0$; (b) $N = 16$, $\phi_v = 0.6$, $\epsilon_{AB} = 0$; (c) $N = 32$, $\phi_v = 0.6$, $\epsilon_{AB} = 0$; (d) $N = 64$, $\phi_v = 0.6$, $\epsilon_{AB} = 0$; (e) $N = 16$, $\phi_v = 0.8$, $\epsilon_{AB} = 0$; (f) $N = 16$, $\phi_v = 0.8$, $\epsilon_{AA} = \epsilon_{BB} = 0$.

is neglected, apart from forbidding immediate reversals of the walk. The linear dimensions of such nonreversal random walks (NRRW) are[55]

$$\langle R^2\rangle_{\mathrm{NRRW}} = \frac{3}{2}(N-1) - \frac{5}{8}\left(1 - \frac{1}{5^{N-1}}\right) \qquad (39a)$$

$$\langle R^2_{\mathrm{gyr}}\rangle_{\mathrm{NRRW}} = \frac{1}{4}\,\frac{(N-1)(N+1)}{N} - \frac{5}{16}\,\frac{N-1}{N} + \frac{5}{32}\,\frac{N-1}{N^2} - \frac{5}{128}\,\frac{1}{N^2}(1 - 1/5^{N-1}) \qquad (39b)$$

It is seen that even for $\phi_v \to 0$ the linear dimensions of the coils seem to be somewhat more expanded than according to eq 39, see Figure 13. Figures 12 and 13 show that for $\phi_v = 0.8$ all our chains have linear dimensions still rather similar to self-avoiding walks in the dilute limit $\phi_v \to 1$, and also for $\phi_v \leq 0.6$ one always has to reach a regime of $N \gtrsim 30$ in order that $\langle R^2\rangle \propto N$ and $\langle R^2_{\mathrm{gyr}}\rangle \propto N$ hold. Although our systems are fairly concentrated, due to the shortness of the chains excluded volume effects are still present, and this must be taken into account when one compares the results of the Monte Carlo calculations to

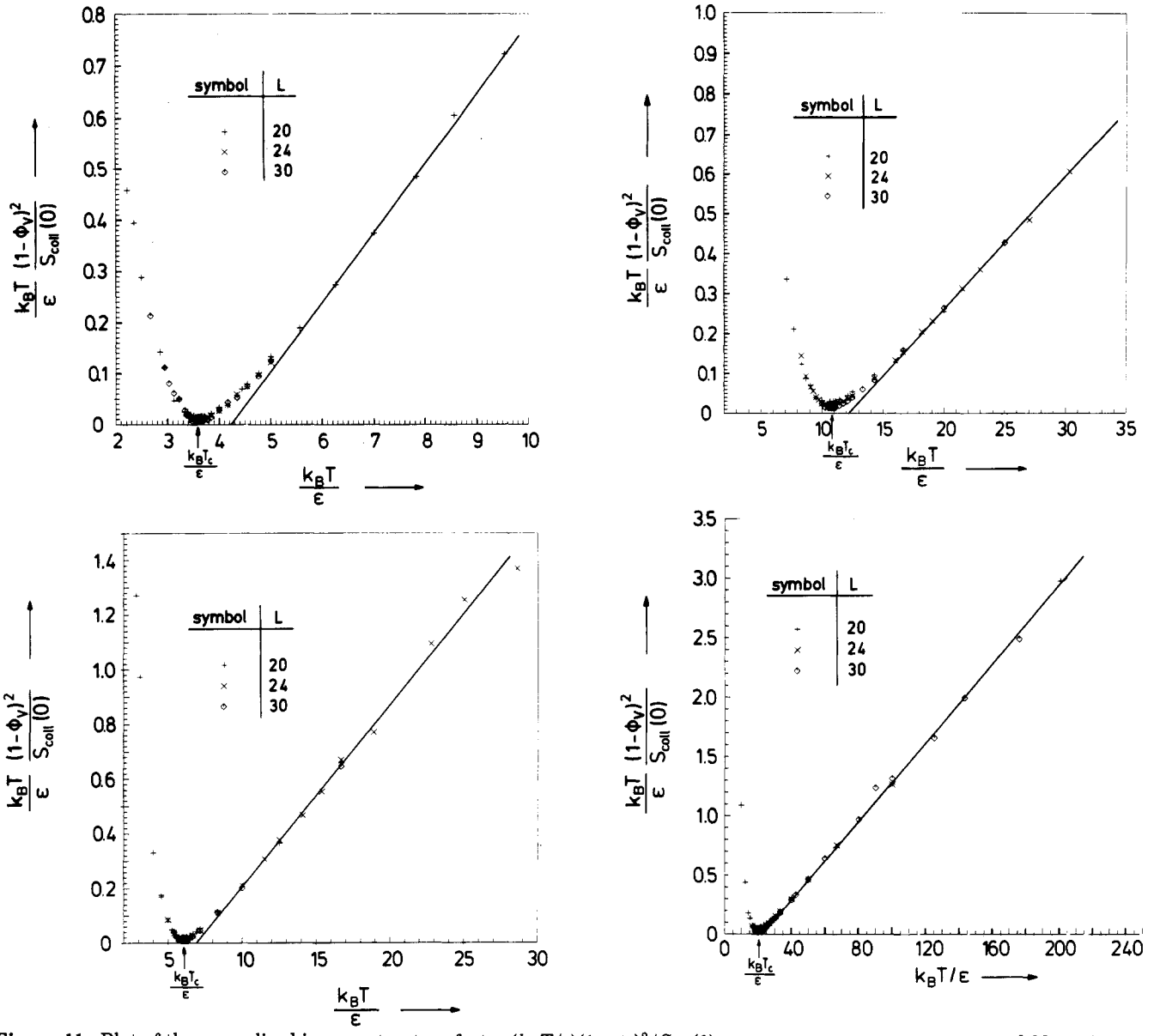


**Figure 11.** Plot of the normalized inverse structure factor $(k_BT/\epsilon)(1-\phi_v)^2/S_{coll}(0)$ versus temperature at $\phi_v = 0.6$ and $N = 8$ (a, top left), $N = 16$ (b, bottom left), $N = 32$ (c, top right), and $N = 64$ (d, bottom right). Different symbols denote different linear dimensions $L$ of the cubic box used in the simulations. Actual critical temperatures were obtained from an analysis as described in section 2.

the theoretical predictions, which usually are based on asymptotic relations ($\langle R^2\rangle \propto N$, $\langle R^2_{gyr}\rangle \propto N$) only.

Recently the accuracy of dynamic Monte Carlo simulations of polymer chains on lattices, as done here, has been questioned on the ground that such algorithms are not strictly ergodic: certain "locked configurations" do not contribute to the averages.[56] The consistency of the results of the present work with other calculations,[50-54] which apply different techniques (the "slithering snake" or "reptation" technique[34] is applied in ref 53, while ref 54 also applies local dynamic motions similar to the present case but includes more types of motions), can be taken as evidence that the problems noted in ref 56 are negligible for our purposes, at least for the restricted range of chain lengths considered.

The main interest of the present study, of course, is to consider whether the interactions between the chains affect their linear dimensions as well. Figure 14 shows that due to the attractive interactions there is indeed a noticeable *contraction* of chain linear dimensions. If one works at asymmetric concentrations ($\phi_A \neq \phi_B$), this contraction is more pronounced for the minority chains, as expected, because then intrachain contacts are favorable in order to lower their energy.

We emphasize that the behavior seen in Figure 14 is not an artifact of a too short length of the chains, but persists in the limit $N \to \infty$, in which case the temperature scale is moved toward smaller and smaller values of $\epsilon/k_BT$, of course. Figure 15 shows the radii for $\phi_A/\phi_B = 9$ as in Figure 14 for various $N$, the temperature always being adjusted such that $\phi_A = \phi^{(1)}_{coex}$ and $\phi_B = \phi^{(2)}_{coex}$. It is seen that the difference in radii between the majority and minority species is largest for $N \to \infty$.

The change of chain linear dimensions with temperature and relative concentration $\phi_A/(\phi_A + \phi_B)$ clearly is an effect which goes beyond the simple theories outlined in section 3. Even if we neglect these variations, we should take into account the enhancement of the linear dimensions with increasing vacancy concentration $\phi_v$, shown in Figures 12 and 13, since the state of the system at $\epsilon/k_BT = 0$ acts as a kind of "reference state", relative to which we consider the effects of interactions and the entropy of A–B mixing.

A rather straightforward extension of the standard formulation of the statistical mechanics of binary polymer mixtures[15-17] can be based on the random phase approx-

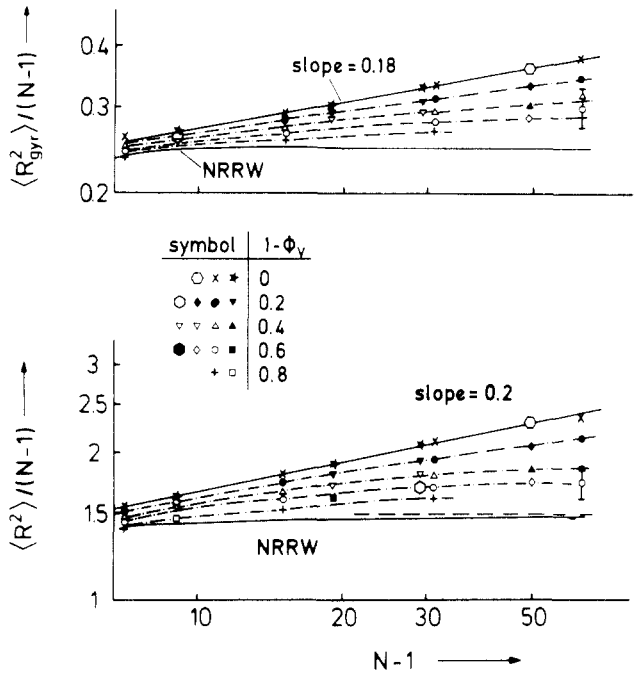


**Figure 12.** Log–log plot of the normalized gyration radius square $\langle R^2_{gyr}\rangle/(N-1)$, upper part, and the normalized squared end-to-end distance $\langle R^2\rangle/(N-1)$, lower part, versus the number of bonds $N-1$ per chain for various concentrations of vacancies $\phi_v$ as indicated and the athermal case ($\epsilon/k_BT = 0$). Data for $N$ = 10, 20, and 30 are due to De Vos and Bellemans[50,51] and Okamoto[53] while data for $N = 50$ are due to Olaj and Lantschbauer[53] (at $1-\phi_v = 0$, 0.4, 0.6) and Okamoto[54] (at $1-\phi_v = 0$, 0.2). Dash-dotted curves are guides to the eye only. Solid curves represent simple power laws (for $1-\phi_v = 0$, the exponents being indicated in the figure) and the NRRW approximation, eq 39, respectively. Errors are always smaller than the sizes of the symbols, except for the point $N = 64$, $1-\phi_v = 0.6$, where the error bar is given.

imation (RPA) of de Gennes[28] for the collective structure function $S_T(\vec{k})$ [note that $S_T(\vec{k}) = S_{coll}(\vec{k})/4$ if $S_{coll}(\vec{k})$ is defined as done in eq 6 and 7]

$$S_T^{-1}(\vec{k}) = \frac{1}{\phi_A S_a(\vec{k})} + \frac{1}{\phi_B S_B(\vec{k})} - 2\chi \qquad (40)$$

where $\phi_A + \phi_B = 1$ for a binary mixture, with $S_A(\vec{k})$ and $S_B(\vec{k})$ being the single-chain structure factors of A chains and B chains, respectively. The standard assumption now involves Gaussian statistics and expresses then $S_A(\vec{q})$ and $S_B(\vec{q})$ in terms of the associate Debye functions, with $\langle R^2_{gyr}\rangle_A = \sigma_A^2 N_A/6$, $\langle R^2_{gyr}\rangle_B = \sigma_B^2 N_B/6$, $\sigma_A$ and $\sigma_B$ being the sizes of effective segments of the two chains, and $N_A$ and $N_B$ being the chain lengths. It is this approximation which we wish to avoid, and hence we put

$$S_A(\vec{k}) = N_A\left(1 - \frac{\langle R^2_{gyr}\rangle_A k^2}{3}\right);$$

$$S_B = N_B\left(1 - \frac{\langle R^2_{gyr}\rangle_B k^2}{3}\right); \quad k \to 0 \qquad (41)$$

without implying anything about $\langle R^2_{gyr}\rangle_A$ or $\langle R^2_{gyr}\rangle_B$. This yields

$$S_T^{-1}(\vec{k}) = \frac{1}{\phi_A N_A} + \frac{1}{\phi_B N_B} - 2\chi + \frac{1}{3}\left[\frac{\langle R^2_{gyr}\rangle_A}{\phi_A N_A} + \frac{\langle R^2_{gyr}\rangle_B}{\phi N_B}\right]k^2 \qquad (42a)$$

which simplifies in the symmetric case (using $\phi_A = \phi$, $\phi_B = 1-\phi$, $N_A = N_B = N$) to

$$S_T^{-1}(\vec{k}) = \frac{1}{\phi(1-\phi)N} - 2\chi + \frac{1}{3}\frac{\langle R^2_{gyr}\rangle}{\phi(1-\phi)N}k^2 \qquad (42b)$$

It is obvious that inclusion of excluded volume via a more general behavior of $\langle R^2_{gyr}\rangle$ *does not change* $S_T^{-1}(k=0)$; only terms of order $k^2$ get affected within the RPA. As a consequence, however, also the coefficient of the gradient square term in the effective Ginzburg–Landau functional[15-17,46] gets changed

$$\frac{\Delta\mathcal{F}}{k_BT} = \int d\vec{x}\left\{f[\phi(x)] + \frac{1}{6}\left[\frac{\langle R^2_{gyr}\rangle_A}{\phi_A N_A} + \frac{\langle R^2_{gyr}\rangle_B}{\phi_B N_B}\right][\nabla\phi]^2\right\} \qquad (43a)$$

where in the asymmetric case the free energy density corresponding to eq 42a is the same as eq 3

$$f(\phi) = \frac{\phi_A \ln \phi_A}{N_A} + \frac{\phi_B \ln \phi_B}{N_B} + \chi\phi_A\phi_B \qquad (43b)$$

while in the symmetrical case we can write $f(\phi) = [\phi \ln \phi + (1-\phi)\ln(1-\phi)]/N + \chi[\phi(1-\phi)]$ and

$$\frac{\Delta\mathcal{F}}{k_BT} = \int d\vec{x}\left\{f[\phi(\vec{x})] + \frac{1}{6}\frac{\langle R^2_{gyr}\rangle}{\phi(1-\phi)N}[\nabla\phi(\vec{x})]^2\right\} \qquad (43c)$$

A behavior of $\langle R^2_{gyr}\rangle$ different from the simple Gaussian behavior $\langle R^2_{gyr}\rangle = \sigma^2 N/6$ does affect the mapping of the long-wavelength properties of the polymer mixture to the equivalent medium-range Ising model[46] as well as the validity of mean-field approximations according to the Ginzburg criterion.[15,29] Since the free energy density of an Ising model in mean-field approximation is $f_{Ising} = \phi \ln \phi + (1-\phi)\ln(1-\phi) + 2(T_c/T)\phi(1-\phi)$

$$\frac{\Delta\mathcal{F}_{Ising}}{k_BT} = \int dx\left\{f_{Ising}[\phi(\vec{x})] + \frac{1}{2}r^2[\nabla\phi(\vec{x})]^2\right\} \qquad (44)$$

with $r$ being the interaction range of the Ising model, we find

$$\Delta\mathcal{F} \equiv \Delta\mathcal{F}_{Ising}/N \qquad r^2 \equiv \frac{\langle R^2_{gyr}\rangle}{3\phi(1-\phi)} \qquad (45)$$

$$N\chi \equiv 2T_c/T$$

Hence it is seen that the gyration radius plays the role of an effective interaction range. Now for a medium-range Ising model mean-field approximations are valid as long as

$$r^d(1 - T/T_c)^{(4-d)/2} \gg 1 \qquad d < 4 \qquad (46)$$

where $d$ represents spatial dimensionality. According to eq 45 this is translated into the polymer case replacing $r^d$ by $(1/N)\langle R^2_{gyr}\rangle^{d/2}$, if we disregard the numerical factor $3\phi(1-\phi)$, which is $^3/_4$ at the critical point. Hence the mean-field approximation for the polymer mixture should be valid as long as (for $d = 3$)

$$\frac{1}{N}\langle R^2_{gyr}\rangle^{3/2}(1 - T/T_c)^{1/2} \gg 1 \qquad (47)$$

The variable on the left-hand side of the Ginzburg criterion is also the appropriate variable to describe the crossover from mean-field to Ising-like critical behavior; e.g., for the order parameter we obtain

$$m = (1 - T/T_c)^{1/2}\tilde{f}_m\{(1 - T/T_c)\langle R^2_{gyr}\rangle^3/N^2\} \qquad (48)$$

where the scaling function $\tilde{f}_m(\zeta)$ must behave as $\tilde{f}_m(\zeta\to\infty) = \sqrt{3}$, in order that for $N \to \infty$ eq 33 is reproduced, while

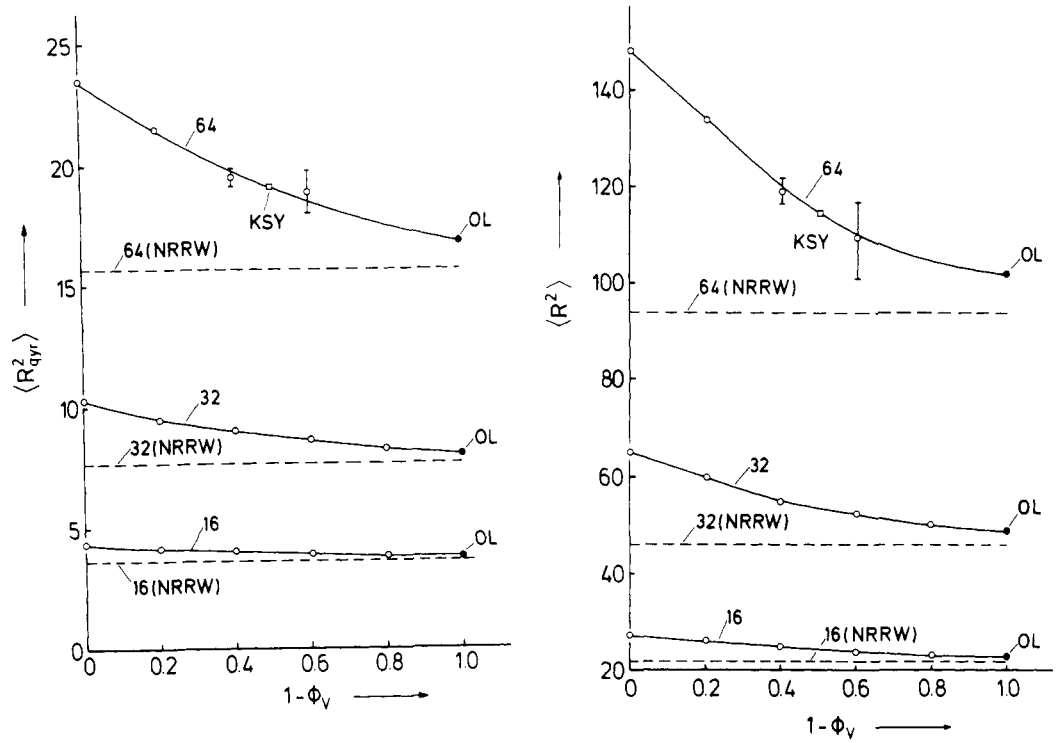


**Figure 13.** Plot of mean-square gyration radius (a, left) and mean-square end-to-end distance (b, right) versus monomer concentration $1 - \phi_v$ in the noninteracting case ($\epsilon/k_BT = 0$). Error bars are only given if they exceed the size of the points, curves are guides to the eye only, and broken horizontal lines are the predictions based on eq 39. Parameters of the curves are the chain lengths $N$. Points denoted by KSY are taken from ref 54, while points denoted by OL are obtained by extrapolating results of ref 52 to the chain lengths used here. Note that these points for $\phi_v = 0$ may have a small systematic error because the sampling technique of ref 52 uses nonmonodisperse polymer chain systems.

$\tilde{f}_m(\zeta \to 0) \propto \zeta^{\beta-0.5}$, in order that eq 14 is reproduced for $T \to T_c$. For $\langle R^2_{gyr}\rangle = \sigma^2 N/6$ eq 48 reduces to the crossover scaling description of ref 36, of course. Note that the factor $1/N$ in eq 47 can be simply interpreted as $\chi_c$, the Flory–Huggins parameter at the critical point (cf. eq 45). This becomes obvious if we rewrite eq 42b as

$$S_T^{-1}(\vec{k}) = 2\chi_c\left(1 - \frac{\chi}{\chi_c}\right)[1 + \xi^2 k^2]$$

$$\xi = \frac{1}{3^{1/2}}\langle R^2_{gyr}\rangle^{1/2}\left(1 - \frac{\chi}{\chi_c}\right)^{-1/2} \qquad (49)$$

with $\xi$ being the correlation length of concentration fluctuations. The condition that the mean-square concentration fluctuation in a correlation volume is much smaller than the mean-square order parameter then also yields eq 47 or alternatively $\chi_c\langle R^2_{gyr}\rangle^{3/2}(1 - \chi/\chi_c)^{1/2} \gg 1$.

Unfortunately, the considerations presented in eq 40–49 seem not to be consistent with the critical behavior observed in the simulations. This is seen in Figure 16 where the results for $m$ in the critical region are plotted in such a way that the results for different chain lengths should collapse on a single function, related to the scaling function $\tilde{f}_m$. The crossover scaling implied by eq 48 does not work, whether we use the actual results for $\langle R^2_{gyr}\rangle$ (Figures 12 and 13) or the asymptotic for $\langle R^2_{gyr}\rangle = \sigma^2 N/6$ valid for $N \to \infty$ and $1 - \phi_v \neq 0$.

More work is necessary to understand this discrepancy: possibly recent renormalization group theories[57-59] dealing with polymer mixtures in dilute and semidilute solutions can explain the present data,[60] although in a strict sense these theories are valid for nonconcentrated solutions only ($1 - \phi_v \lesssim 0.1$). Qualitatively, one has to partition the chains into "blobs", the size of which depends on the vacancy concentration $\phi_v$. Inside one blob, the chain configuration is swollen, and basically there are no monomers of other chains. This leads to an effective "renormalized" Flory–Huggins parameter $\chi$. We intend to check these concepts in future work.

## 5. Conclusions

For the first time in the present work a Monte Carlo investigation of the thermodynamics of the Flory–Huggins lattice model of polymer mixtures including vacancies has been given. Our results show that for the simple cubic lattice the Flory approximation for the critical temperature of the model fails rather badly. The Guggenheim approximation though, somewhat better, is still rather inaccurate (Figure 5). We interpret the inaccuracies of these theories in terms of an overestimation of the number of contacts that monomers of a given chain have with monomers of other chains. In contrast, we are proposing that at $\epsilon/k_BT = 0$ for symmetrical mixtures ($N_A = N_B = N$) the entropy of A–B mixing expression $\Delta S/k_B = [\phi_A \ln \phi_A + \phi_B \ln \phi_B - (1 - \phi_v) \ln (1 - \phi_v)]/N$ is exact, because $\Delta S$ simply counts the ways in which in each polymer–vacancy configuration the "unlabeled" polymer chains can be "labeled" as A or B consistent with a given volume fraction $\phi_A$ of A chains and $\phi_B$ of B chains. The complicated problem of enumerating the number of ways in which the polymer chains of length $N$ can be placed on the lattice consistent with a given volume fraction $\phi_v$ of vacancies is not involved in the "labeling" problem, and hence the entropy associated with this chain configurational statistics cancels out from $\Delta S$. A consequence of the fact that the A–B mixing part of the entropy is exact is also the fact that the equation of state in the noninteracting limit simply is $m = \tanh(N\Delta\mu/2k_BT)$, where $\phi_A = [(1 - \phi_v)(1 + m)]/2$ and $\phi_B = [(1 - \phi_v)(1 - m)]/2$; this is so because then in the grandcanonical ensemble each chain can be "labeled" independently of each other chain, with probabilities $p_A =$

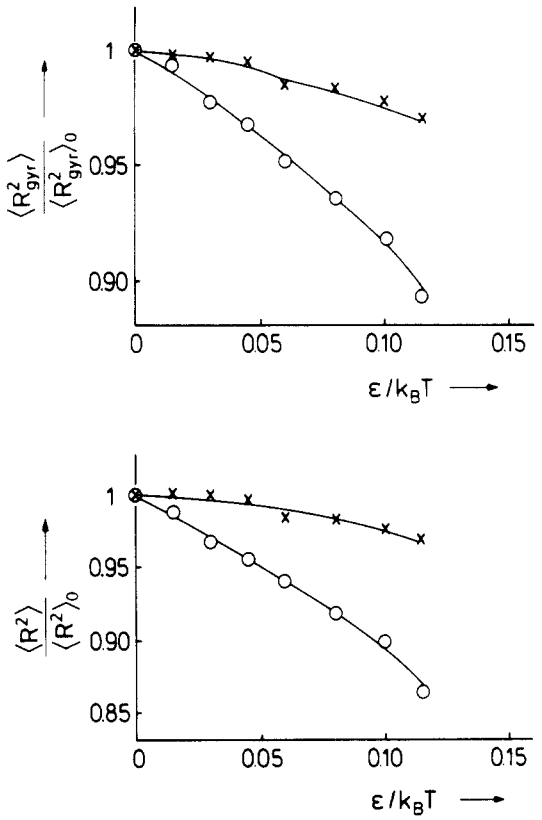


**Figure 14.** Plot of the mean-square gyration radius $\langle R^2_{gyr}\rangle$ (upper part) and the mean-square end-to-end distance $\langle R^2\rangle$ (lower part) at constant $\phi_A$ versus inverse temperature, $\epsilon/k_BT$, for $N = 32$ and $\phi_v = 0.6$. Both radii are normalized by their values at $\epsilon/k_BT = 0$. The crosses refer to the majority component ($\phi_A/(1 - \phi_v) = 0.9$), the circles to the minority component ($\phi_B/(1 - \phi_v) = 0.1$). Curves are guides to the eye only. Note that the largest $\epsilon/k_BT$ shown corresponds to results taken at the coexistence curve (still larger $\epsilon/k_BT$ would correspond to metastable states inside the two-phase coexistence region).

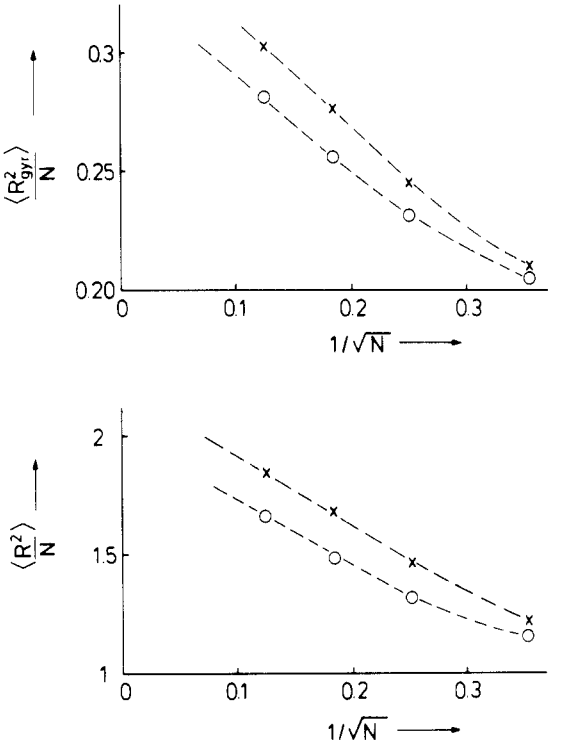


**Figure 15.** Plot of the mean-square gyration radius $\langle R^2_{gyr}\rangle$ normalized per chain length $N$ (upper part) and of the mean-square end-to-end distance $\langle R^2\rangle$ normalized per chain length (lower part) as function of $1/\sqrt{N}$, for $\phi_A/(1 - \phi_v) = 0.9$, $\phi_B/(1 - \phi_v) = 0.1$, $\phi_v = 0.6$, and $\epsilon/k_BT$ chosen such that the state is at the coexistence curve for each value of $N$.

$\exp(N\Delta\mu/2k_BT)/[\exp(N\Delta\mu/2k_BT) + \exp(-N\Delta\mu/2k_BT)]$ and $p_B = \exp(-N\Delta\mu/2k_BT)/[\exp(N\Delta\mu/2k_BT) + \exp(-N\Delta\mu/2k_BT)]$, with $\Delta\mu$ being the chemical potential difference between A and B monomers. Now the order parameter $m = (\phi_A - \phi_B)/(1 - \phi_v) = p_A - p_B$. This property has also been verified directly by the simulations (Figure 7). We have also verified that the actual number of interchain contacts that monomers of one chain have is considerably less than the estimates resulting from the Flory approximation ($zN$, $z$ being the coordination number) or Guggenheim approximation ($(z - 2)N + 2$), see Figure 10.

We also have studied the coexistence curve (obtained from the order parameter for $\Delta\mu = 0$) and the collective structure factor $S_{coll}(\vec{k}=0)$, and we have compared them to the Flory and the Guggenheim approximations. We find that the actual coexistence curve has not the parabolic shape resulting from such approximations but is considerably flatter (Figure 6), reflecting the Ising critical exponent $\beta$. Similarly, a plot of $S^{-1}_{coll}(\vec{k}=0)$ versus temperature near the critical point does not vanish linearly but rather in a curved fashion, reflecting the Ising critical exponent $\gamma$, although in a broad regime of temperatures a linear variation with temperature is a reasonable approximation (Figure 11). While these results are consistent with current theoretical expectations, the failure of our results to show the expected crossover scaling behavior (Figure 16) is unexpected.

Particular attention has also been paid to the linear dimensions of the chains (Figures 12–15). In the noninteracting limit our results are in full agreement with various earlier investigations, extending them over a more complete range of vacancy concentration and chain lengths. It is shown that even for fairly concentrated systems there are still short-scale excluded volume effects present, the linear dimensions always being distinctly longer than those of the nonreversal random walk approximation (Figures 12 and 13). In the interacting case the chain linear dimensions get somewhat reduced when $\epsilon/k_BT$ increases (Figure 14). This reduction of linear dimensions is more pronounced for the minority component than for the majority component; the relative difference between majority and minority radii goes to a finite limit at the coexistence curve for $N \to \infty$.

Are there any consequences for the use of the Flory–Huggins approximation in the interpretation of experiments? We feel that the Flory–Huggins free energy expression may still be a useful "working formula" to "fit" real data but one should be careful in attributing too much physical meaning to the dependence of the Flory–Huggins parameter on temperature and volume fractions; part of these dependences are due to the inaccuracies of the underlying approximations. This is clearly revealed by Figures 8 and 9, where the numerical results for the equation of state (Figure 7) were treated as "given experimental data" and estimates for $\chi$ were extracted from them by using the Flory equation of state or the Guggenheim equation of state, respectively. The resulting effective interaction parameter $\epsilon_{eff}/k_BT = \chi_{eff}(\phi_A,T)/z(1 - \phi_v)$ differs from the actual $\epsilon/k_BT$; not only is it offset by a temperature-dependent factor, but there are also spurious dependences on $\phi_A$, $\phi_v$, and $N$.

The advances described in the present work did require substantial amounts of computing time, and rather special simulation techniques had to be used (grandcanonical sampling technique, finite-size scaling, cumulant inter-

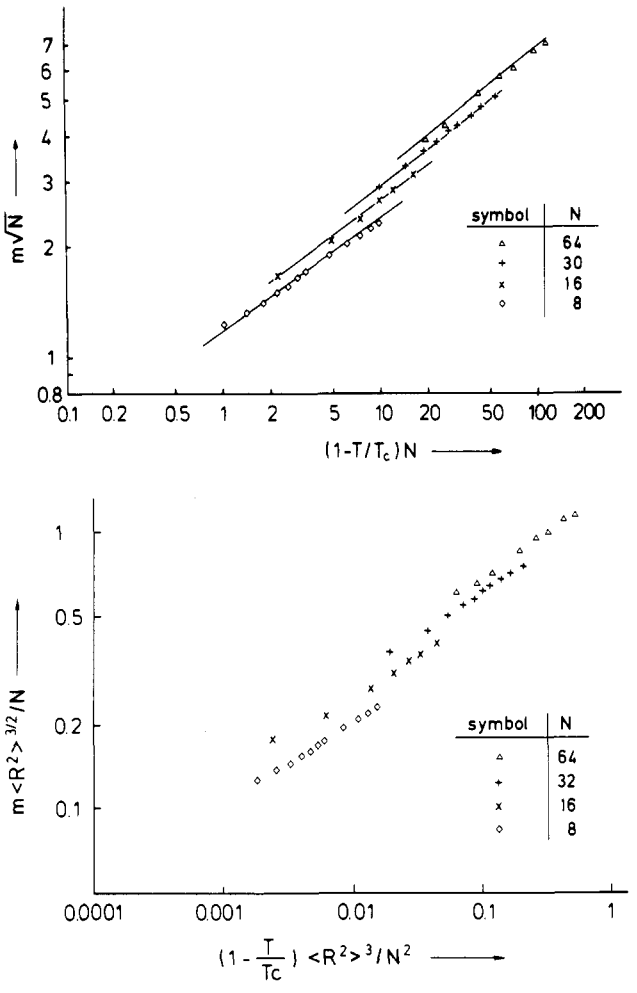


**Figure 16.** Crossover scaling plot of the order parameter for $\phi_v = 0.6$: (a, top) $mN^{1/2}$ is plotted as a function of $(1 - T/T_c)N$ for four different chain lengths $N$ as indicated. Only points not affected by finite-size rounding are included in this figure. Straight lines indicate an order parameter exponent of about $\beta \approx 0.32 \pm 0.01$. Note that according to eq 48 the curves for various values of $N$ should all be parts of a single-valued function of $(1 - T/T_c)N$. (b, bottom) $m\langle R^2\rangle^{3/2}/N$ plotted as a function of $(1 - T/T_c)\langle R^2\rangle^3/N^2$ to show that also with this choice of scaling variables the data do not collapse on a single curve.

section methods, etc.). Thus the extension of the present study to truly realistic models is not straightforward (where various types of asymmetries need to be included, off-lattice chains should be treated with realistic rotational potentials and interchain potentials representing the steric effects of various sidegroups, etc.). But there is no reason to assume that the inaccuracies that already are occurring in the standard Flory–Huggins treatment of the very simplest model, as revealed here, become less severe when one moves along to more complicated situations. Instead we hope that the present work may provide some guidance for the improvement of these theoretical approaches and that it also will stimulate careful experiments to yield more complete information on the thermodynamic properties of real polymer mixtures. A very promising approach to understand phase separation of polymer mixtures in dilute and semidilute solution is the renormalization group approach;[57-59] thus an extension of the present work to smaller polymer concentrations seems very desirable and will be presented in future work. After this manuscript had been essentially completed, Leibler[60] has informed us that the theory[59] even can account for the chain length dependence of critical amplitudes observed in our previous work[36] on very concentrated solutions ($\phi_v = 0.2$). We are planning to perform additional calculations for small values of $1 - \phi_v$ and to carry out a detailed comparison to the theory and pertinent experiments in our future work.

**Acknowledgment.** This work was supported in part by the Deutsche Forschungsgemeinschaft, Sonderforschungsbereich 41. We acknowledge useful discussions with K. Kremer, L. Leibler, and L. Schäfer.

## References and Notes

(1) Flory, P. J. *Principles of Polymer Chemistry*; Cornell University Press: Ithaca, 1953.
(2) Huggins, M. *J. Am. Chem. Soc.* **1942**, *64*, 1712; *J. Phys. Chem.* **1942**, *46*, 151; *J. Chem. Phys.* **1941**, *9*, 440.
(3) Flory, P. J. *J. Chem. Phys.* **1942**, *10*, 51.
(4) Staverman, A. J. *Recl. Trav. Chim.* **1941**, *60*, 640. Staverman, A. J.; Van Santen, J. H. *Recl. Trav. Chim.* **1941**, *60*, 76.
(5) Tompa, H. *Polymer Solutions*; Butterworths: London, 1956.
(6) Scott, R. L. *J. Chem. Phys.* **1949**, *17*, 279.
(7) Koningsveld, R.; Kleintjens, L. A.; Schoffeleers, H. M. *Pure Appl. Chem.* **1974**, *39*, 1.
(8) Koningsveld, R.; Kleintjens, L. A.; Nies, E. *Croat. Chim. Acta* **1987**, *60*, 53.
(9) Sanchez, I. C. *Macromolecules* **1984**, *17*, 967.
(10) Zeman, L.; Patterson, D. *Macromolecules* **1972**, *5*, 513.
(11) Solc, K. *Macromolecules* **1986**, *19*, 1166.
(12) Guggenheim, E. A. *Proc. R. Soc. (London)* **1945**, *A183*, 203, 231.
(13) Miller, A. R. *Proc. Cambridge Philos. Soc.* **1943**, *39*, 54.
(14) Bawendy, M. G.; Freed, K. F.; Mohanty, U. *J. Chem. Phys.* **1986**, *84*, 7036.
(15) de Gennes, P.-G. *J. Chem. Phys.* **1981**, *72*, 4756.
(16) Pincus, P. *J. Chem. Phys.* **1981**, *75*, 1996.
(17) Binder, K. *J. Chem. Phys.* **1983**, *79*, 6387; *J. Colloid Polym. Sci.* **1987**, *265*, 273.
(18) Binder, K.; Schichtel, T. *Macromolecules* **1987**, *20*, 1671.
(19) Helfand, E.; Tagami, Y. *J. Polym. Sci* **1971**, *B9*, 741; *J. Chem. Phys.* **1971**, *56*, 3592; *J. Chem. Phys.* **1972**, *57*, 1812.
(20) Helfand, E. *J. Chem. Phys.* **1975**, *62*, 999; *J. Chem. Phys.* **1975**, *63*, 2792.
(21) Helfand, E.; Sapse, M. *J. Chem. Phys.* **1975**, *62*, 1327.
(22) Helfand, E.; Weber, T. A. *Macromolecules* **1976**, *9*, 311.
(23) Joanny, J. F.; Leibler, L. *J. Phys. (Paris)* **1978**, *39*, 951.
(24) Binder, K.; Frisch, H. L. *Macromolecules* **1984**, *17*, 2928.
(25) Hong, K. M.; Noolandi, J. *Macromolecules* **1981**, *14*, 727; *Macromolecules* **1983**, *16*, 1083. Noolandi, J.; Hong, K. M. *Macromolecules* **1982**, *15*, 482.
(26) Leibler, L. *Macromolecules* **1980**, *13*, 1602.
(27) Sanchez, I. C.; Lacombe, R. H. *J. Phys. Chem.* **1976**, *80*, 2352; *Macromolecules* **1978**, *11*, 1145. Lacombe, R. H.; Sanchez, I. C. *J. Phys. Chem.* **1976**, *80*, 2568.
(28) de Gennes, P.-G. *Scaling Concepts in Polymer Physics*; Cornell University Press: Ithaca, 1979.
(29) de Gennes, P.-G. *J. Phys. Lett. (Paris)* **1977**, *38*, L441. Joanny, J. F. *J. Phys. A: Math. Gen.* **1978**, *A11*, L117.
(30) Herkt-Maetzky, C.; Schelten, J. *Phys. Rev. Lett.* **1983**, *51*, 896.
(31) Yang, H.; Shibayama, M.; Stein, R. S.; Han, C. C. *Polym. Bull. (Berlin)* **1984**, *12*, 7. Shibayama, M.; Yang, H.; Stein, R. S.; Han, C. C. *Macromolecules* **1985**, *18*, 2179.
(32) *Monte Carlo Methods in Statistical Physics*; Binder, K., Ed.; Springer: Berlin, 1979.
(33) *Applications of the Monte Carlo Method in Statistical Physics*; Binder, K., Ed.; Springer: Berlin, 1984.
(34) Baumgärtner, A. in ref 33, Chapter 5.
(35) Sariban, A.; Binder, K.; Heermann, D. W. *J. Colloid Polym. Sci.* **1987**, *265*, 424; *Phys. Rev. B: Condens. Matter* **1987**, *35*, 6873.
(36) Sariban, A.; Binder, K. *J. Chem. Phys.* **1987**, *86*, 5853.
(37) For the problem of only one sort of chains on a lattice, similar tests were performed in ref 38, where it was found that the Flory[1] approximation was not providing a good fit to the data while the formula due to Huggins[2] and Guggenheim[12]–Miller[13] performed distinctly better. However, one expects all these theories to break down when one enters the "semidilute" concentration regime.[28]
(38) Okamoto, H.; Bellemans, A. *J. Phys. Soc. Jpn.* **1979**, *47*, 955. Dickman, R.; Hall, C. K. *J. Chem. Phys.* **1986**, *85*, 3023.
(39) Fisher, M. E.; Barber, M. N. *Phys. Rev. Lett.* **1972**, *28*, 1516. Barber, M. N. In *Phase Transitions and Critical Phenomena*; Domb, C., Lebowitz, J. L., Eds.; Academic: New York, 1983; Vol. 8, Chapter 2.
(40) Binder, K. *Z. Physik* **1981**, *B43*, 119; *Ferroelectrics* **1987**, *73*, 43.

(41) Binder, K.; Nauenberg, M.; Privman, V.; Young, A. P. *Phys. Rev. B: Condens. Matter* **1985**, *B31*, 1498.
(42) Rosenbluth, M.; Rosenbluth, A. *J. Chem. Phys.* **1955**, *23*, 356.
(43) Note that the three-bond motion creates new bond vectors on the simple cubic lattice.
(44) Stanley, H. E. *An Introduction to Phase Transitions and Critical Phenomena*; Oxford University Press: Oxford, 1971.
(45) Le Guillou, J. C.; Zinn-Justin, J. *Phys. Rev. B: Condens. Matter* **1980**, *B21*, 3976.
(46) Binder, K. *Phys. Rev. A* **1984**, *A29*, 341.
(47) See, for example, eq 4.67 and 4.34 as well as eq 3.30 and 3.37 of ref 5.
(48) Scott, R. L. *J. Chem. Phys.* **1949**, *17*, 268.
(49) Schwahn, D.; Mortensen, K.; Yee-Madeira, H. *Phys. Rev. Lett.* **1987**, *58*, 1544.
(50) De Vos, E.; Bellemans, A. *Macromolecules* **1974**, *7*, 812.
(51) De Vos, E.; Bellemans, A. *Macromolecules* **1975**, *8*, 651.
(52) Olaj, O. F.; Lantschbauer, W. *Makromol. Chem., Rapid Commun.* **1982**, *3*, 847.
(53) Okamoto, H. *J. Chem. Phys.* **1983**, *79*, 3976.
(54) Kolinski, A.; Skolnick, J.; Yaris, R., preprint.
(55) Domb, C.; Fisher, M. E. *Proc. Cambridge Philos. Soc.* **1958**, *54*, 48.
(56) Caracciolo, S.; Sokal, A. D. *J. Phys. A: Math. Gen.* **1986**, *A19*, L797. Madras, N.; Sokal, A. D. *J. Stat. Phys.*, in press.
(57) Joanny, J. F.; Leibler, L.; Ball, R. *J. Chem. Phys.* **1984**, *81*, 4640.
(58) Schäfer, L.; Kappeler, Ch. *J. Phys (Paris)* **1985**, *46*, 1853.
(59) Broseta, D.; Leibler, L.; Joanny, J. F. *Macromolecules*, in press.
(60) Leibler, L., private communication.

# Dimensions of a Polymer Chain in a Mixed Solvent

**J. J. Magda,* G. H. Fredrickson, R. G. Larson, and E. Helfand**

*AT&T Bell Laboratories, Murray Hill, New Jersey 07974.* *Received July 21, 1987*

ABSTRACT: The equilibrium behavior of a flexible polymer in a binary solvent mixture is investigated via Monte Carlo simulation. The mixed solvent is modeled as an Ising fluid occupying the sites of a simple cubic lattice, with the polymer described as a self-avoiding random walk on the same lattice. The solvent has a critical consolute point, and the polymer preferentially adsorbs the better solvent component. A coupling between preferential adsorption and the solvent correlations present near the consolute temperature of the solvent causes the chain to contract, as predicted by Brochard and de Gennes. However, preferential adsorption also causes chain contraction far from the critical temperature. At large values of preferential adsorption, the chain contracts below the dimensions it would have in either of the pure solvent components.

## I. Introduction

Our understanding of the equilibrium properties of linear polymers in one-component solvents is very well developed. On the basis of mean field theories, such as the Flory–Huggins theory,[1] and more sophisticated renormalization group theories,[2,3] experiments on dilute polymer solutions can be quantitatively interpreted. As a consequence, recent theoretical efforts have been focused on less mature areas such as semidilute solution statics and dynamics, the dynamics of entanglements, and interfacial phenomena.

A problem that has received surprisingly little attention is the configurational statistics and thermodynamic properties of polymers in mixed solvents. Because a polymer chain may preferentially adsorb one of the solvent components, such systems can possess inhomogeneities not found in solutions of a polymer in a single-component solvent. Among the few theoretical treatments of this problem are the Shultz–Flory theory,[4] a type of mean field theory, and the Brochard–de Gennes theory,[5-7] which deals with the particular case of the solvent mixture being near a critical point. A related problem is the collapse of a large polymer in a good solvent upon the addition of smaller polymers incompatible with the longer chain.[8-13] The Brochard–de Gennes theory makes an interesting prediction for a polymer in a mixture of two good solvents, where the affinities of the macromolecule for the two solvent components differ substantially. The prediction is that the polymer will adopt collapsed configurations as the critical temperature $T_c$ of the solvent mixture is approached, even though it would be swollen in either of the pure component solvents at the same temperature.

In contrast to the Flory–Huggins theory for one-component solvents, the theories for mixed solvents have not been subjected to extensive experimental tests. In part, this is due to the difficulty in independently varying a particular parameter such as the preferential affinity of the polymer for one of the solvent components, while holding other parameters of the system fixed. Yamakawa[14,15] has pointed out the complications introduced into the analysis of light scattering data by the presence of strong preferential adsorption. Because of such difficulties, experimental studies inconsistent with the Shultz–Flory theory are not particularly convincing.[16,17]

An alternative means of testing the analytical theories for polymers in mixed solvents is through computer simulation.[18] With simulation techniques there is no difficulty in independently varying solvent quality, preferential affinities, or temperature, while holding certain other parameters constant. Furthermore, because information on chain dimensions and correlations is readily accessible, computer simulation methods are ideal for detecting configurational changes, such as the collapse transition predicted by Brochard and de Gennes.

In the present paper we report Monte Carlo lattice simulations of a polymer in a two-component solvent mixture. Various predictions of the Shultz–Flory and Brochard–de Gennes theories are addressed. The organization of the manuscript is as follows. In section II we describe our modification of the conventional Monte Carlo technique to model ternary systems. The relevant theories are briefly reviewed in section III, and the simulation results are presented in section IV. Section V contains a discussion of these results and our conclusions.

## II. Model Ternary System and the Simulation Technique

We consider a single polymer chain in a mixture of two solvents that will be denoted A and B. The state of the system is described by the occupancy of the sites of a simple cubic lattice in three dimensions by A molecules, B molecules, and "monomers" (i.e., the units linked in the polymer chain). The volumes of A, B, and monomer are assumed equal, hence volume fractions and mole fractions

0024-9297/88/2221-0726$01.50/0 